

**Molecular Modelling Studies to Probe the Transcription Regulation of  
CABP4 in Night Blindness**

A thesis submitted in the partial fulfillment of the requirement for the degree of  
MS in Bioinformatics



**By**

**Sana Fatima**

**Master of Science in Bioinformatics**

**Fall 21-MSBI-NUST00000362201**

**Supervised by:**

**Prof. Dr. Ishrat Jabeen**

**School of Interdisciplinary Engineering & Sciences (SINES)**

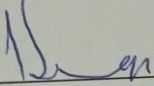
**National University of Sciences & Technology (NUST)**

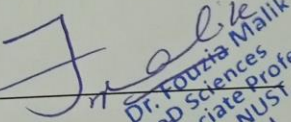
**Islamabad, Pakistan**

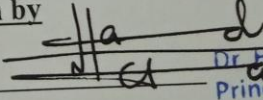
**August, 2023**

## THESIS ACCEPTANCE CERTIFICATE

Certified that the final copy of MS/MPhil thesis written by **Ms. Sana Fatima**, Registration No. **00000362201** of **MS-BI SINES** has been vetted by the undersigned, found complete in all aspects as per NUST Statutes/Regulations, is free of plagiarism, errors, and mistakes, and is accepted as partial fulfillment for the award of MS/MPhil degree. It is further certified that necessary amendments as pointed out by GEC members of the scholar have also been incorporated in the said thesis.

Signature with stamp:   
Name of Supervisor: DR. ISHRAT JABEEN  
Professor  
School of Interdisciplinary  
Engineering & Sciences  
Date: 22-08-23 NUST Sector H-12 Islamabad

Signature of HoD with stamp:   
Date: 23-8-2023  
Dr. Fouzia Malik  
HoD Sciences  
Associate Professor  
SINES - NUST, Sector H-12  
Islamabad

Countersign by   
Signature (Dean/Principal): Dr. Hammad M. Cheema  
Principal & Dean  
Date: 23 AUG 2023 SINES - NUST, Sector H-12  
Islamabad

## CERTIFICATE OF ORGANILITY

I hereby declare that the research work presented in this thesis has been generated by me as a result of my own research work. Moreover, none of its contents are plagiarized or submitted for any kind of assessment or higher degree. I have acknowledged and referenced all the main sources of help in this work.

Sana Fatima

Fall 2021-MS BI 00000362201

---

## ACKNOWLEDGMENT

In the Name of Allah, the Most Merciful, the Most Compassionate all praise be to Allah, the Lord of the worlds; and prayers and peace be upon Mohamed His servant and messenger. First and foremost, I must acknowledge my limitless thanks to Allah, the Ever-Magnificent; the Ever-Thankful, for His help and bless. I am totally sure that this work would have never become truth, without His guidance. I owe a deep debt of gratitude to our school for giving us an opportunity.

I have been able to accomplish this research work and come up with the final dissertation work which is necessary for the award of the degree of MS Bioinformatics. I also would like to express my wholehearted thanks to my family for the generous support they provided me throughout my entire life and particularly through the process of pursuing the master's degree. Because of their unconditional love and prayers, I have the chance to complete this thesis. I would like to take this opportunity to say warm thanks to my friends: Mahnoor Hashmi and Zoya Amjad who have been so supportive along the way of doing my thesis.

I would like to thank my mentor: **Dr. Ishrat Jabeen** for her guidance, support, motivation, and immense knowledge. Once again, I would like to express my sincere gratitude to my advisor Dr. Ishrat Jabeen for the continuous support of my study and related research, for her patience, motivation, and immense knowledge. Her guidance helped me in all the time of research and writing of this thesis. I could not have imagined having a better advisor and mentor for my study. I am very lucky to be her student and I highly appreciate her efforts. Last but not least, my deepest thanks go to all people who took part in making this thesis real.

# TABLE of CONTENTS

<b>ACKNOWLEDGMENT</b> .....	<b>i</b>
<b>LIST OF FIGURES</b> .....	<b>iv</b>
<b>LIST OF TABLES</b> .....	<b>v</b>
<b>Abstract</b> .....	<b>vi</b>
<b>1 Introduction</b> .....	<b>1</b>
1.1 The Vital Role of Calcium Ions (Ca <sup>2+</sup> ) in the Human Body .....	1
1.2 Understanding the Role of Ca <sup>2+</sup> Signaling in Cellular Activities .....	1
1.3 The Impact of Voltage-Gated Calcium Channels (Cav) on Neural Function .....	2
1.4 Ca <sup>2+</sup> Channel Diversity and Functionality .....	2
1.5 The Functional Domains of the L-type Calcium Channels (LTCCs) .....	3
1.6 The Importance of Cav1.4 in Maintaining Normal Transmission of Visual Signals .....	4
1.7 The Role of L-Type Calcium Channels in the Pathogenesis of Various Diseases .....	6
1.8 The Disease Associated with Cav1.4 in the Transmission of Visual Signals.....	6
1.9 Therapeutic Options for Retinal Diseases .....	8
1.9.1 Spliceosome-mediated RNA <i>trans</i> -splicing (SMaRT) .....	8
1.9.2 Gene Therapy .....	9
1.10 Problem Statement .....	9
1.11 Objectives.....	10
<b>2 Literature Review</b> .....	<b>11</b>
2.1 Target Validation of CABP4: A Promising Approach for Night Blindness Treatment.	11
2.2 Rod-Cone Dystrophy.....	11
2.3 Congenital Stationary Night Blindness(CSNB).....	12
2.4 Functional Subunits of Cav1.4.....	13
2.5 The Impact of CABP4 on Channel Activation Voltage.....	15
2.6 Structural Dynamics of CABP4 and Cav1.4 IQ-Motif Domain .....	16

2.7	Interaction between CABP4 and IQ-Motif .....	17
2.8	Emerging Therapeutic Approaches for Retinal Treatment: .....	19
2.9	Spliceosome-mediated RNA trans-splicing (SMaRT).....	20
<b>3</b>	<b>Methodology.....</b>	<b>22</b>
3.1	Biological Regulatory Network (BRN) Construction and its Dynamic Simulation .....	22
3.2	Data Collection.....	23
3.3	Molecular Docking.....	23
3.4	Analysis and Visualization of Docked Complexes .....	24
3.5	Molecular Dynamic Simulation of the Docking Complexes .....	24
<b>4</b>	<b>Results.....</b>	<b>25</b>
4.1	Biological Regulatory Network (BRN) Construction of Light Visual Cascade: .....	25
4.2	Normal Visual Signaling Simulations in Light Response:.....	27
4.3	Biological Regulatory Network (BRN) Construction of Visual Signaling for Dark Response: .....	30
4.4	Normal Visual Signaling Simulations in Dark Response: .....	31
4.5	Biological Regulatory Network (BRN) Construction for Night Blindness: .....	35
4.6	Visual Signaling Simulations in Night-Blindness: .....	36
4.7	Analysis of Stable Structures after Simulation .....	42
4.8	Molecular Docking.....	43
4.9	Interaction between the Molecules of Wild-type Docked Complex .....	44
4.10	Interaction between the Molecules of Mutant Docked Complex.....	46
4.11	MD Simulation Analysis.....	48
<b>5</b>	<b>Discussion .....</b>	<b>52</b>
<b>6</b>	<b>Conclusions.....</b>	<b>54</b>
<b>7</b>	<b>References.....</b>	<b>55</b>

## LIST OF FIGURES

Figure 1: Variability in voltage-gated calcium channels at the genetic level.....	2
Figure 2: Voltage-gated $\text{Ca}^{2+}$ channels mediate signal transduction.....	3
Figure 3: Release of glutamate from the presynaptic membrane of rod cell.....	5
Figure 4: The role of Cav1.4 channel closure in inhibiting signal transmission.....	7
Figure 5: PTM design for the treatment of Retinal diseases.....	8
Figure 6: Illustration of ICDI-mediated closure of $\text{Ca}^{2+}$ -dependent channel Cav1.4.....	9
Figure 7: Disease associations within the calcium domain of CABP4.....	13
Figure 8: Structure of $\alpha 1F$ subunit of Cav1.4.....	14
Figure 9: CABP4 bound to IQ Motif.....	19
Figure 10: Biological Regulatory Network for visual signaling in response to light.....	26
Figure 11: Jimena's dynamic simulation of the visual signaling pathway in light.....	29
Figure 12: Biological Regulatory Network for visual signaling in response to dark.....	31
Figure 13: The results of Jimena's dynamic simulation of the visual signaling pathway in dark.....	33
Figure 14: The results of Jimena's dynamic simulation to reveal the effect of CABP4.....	35
Figure 15: Biological Regulatory Network for visual signaling in night-blindness.....	36
Figure 16: Dynamic simulation of night-blindness.....	37
Figure 17: Dynamic simulation of BRN modertae and hyperactive $\text{Ca}^{2+}$ in night-blindness.....	39
Figure 18: Dynamic simulation of BRN moderate and hyper active CABP4 in night-blindness.....	40
Figure 19: Dynamic simulation of BRN, perturbed with CABP4 and $\text{Ca}^{2+}$ .....	42
Figure 20: The RMSD graph after simulation of Wild-type CABP4, Mutant-CABP4 and IQ-motif.....	43
Figure 21: Visualization of Wild-type CABP4-IQ docked complex using pymol software.....	45
Figure 22: The interaction between the IQ-motif and Wild-type CABP4 in docked complex.....	46
Figure 23: Visualization of Mutant CABP4-IQ docked complex performed using Pymol .....	47
Figure 24: The interaction between the IQ-motif and Mutant CABP4 in docked complex.....	47
Figure 25: Comprehensive analysis of the molecular dynamics (MD) simulation performed on the Wild-type CABP4-IQ and Mutant CABP4-IQ complexes .....	48
Figure 26: The H-bond occupancy for Wild/Mutant docked complexes of CABP4 and IQ motif.....	51

## LIST OF TABLES

Table 1:The PDB IDs and structures of the CABP4 and IQ motif.....	17
Table 2:Parameters values of entities interacting with Ca <sup>2+</sup> and CABP4 before and after simulation.....	28
Table 3:Parameters values of entities interacting with Ca <sup>2+</sup> in dark before and after simulation.....	32
Table 4:Parameters values of entities interacting with CABP4 in dark before and after simulation.....	34
Table 5:Parameters values of entities interacting with Ca <sup>2+</sup> in night blindness before and after simulation.....	38
Table 6:Parameters values of entities interacting with CABP4 in night blindness before and after simulation.....	40
Table 7:Parameters values of entities perturbation CABP4 and Ca <sup>2+</sup> in night blindness before and after simulation.....	41
Table 8:Top 5 Clusters with RMSD,lowest energy score and z-score of Mutant CABP4-IQ docked complex.....	44
Table 9:Top 5 Clusters with RMSD,lowest energy score and z-score of Wild-type CABP4-IQ docked complex.....	44



## Abstract

This research probes the role of  $\text{Ca}^{2+}$  and CABP4 in rod photoreceptors for visual signaling, particularly in varying light conditions. In illuminated situations, rhodopsin activation and closure of the presynaptic Cav1.4 channel are associated with normal visual signaling. However, under low light condition, prolonged opening of the ion channels results in elevated levels of  $\text{Ca}^{2+}$  and calcium-binding proteins specifically CABP4, which prominently regulate Cav1.4 to enhance visual processing efficiency. Mutations in CABP4 have been associated with various diseases, including night blindness, rod-cone dystrophy, and myopia. Thus, to probe the regulation mechanistic of CABP4 and its role in night blindness, Biological Regulatory Network (BRN) has been constructed and simulated. Simulation results of final BRN revealed the model's sensitivity to changes in both CABP4 and  $\text{Ca}^{2+}$  concentration levels and thus, advocate CABP4 along with  $\text{Ca}^{2+}$  modulator as a potential therapeutic option against night blindness.

Furthermore, the regulation of Cav1.4 by CABP4 under both normal and mutated conditions have been simulated. Due to the unavailability of a PDB structure, different homology models of CABP4 have been developed and evaluated. Furthermore, molecular docking and simulations studies were performed to identify favorable binding hypothesis of mutant and wild type CABP4. Our findings indicate that specific residues such as Leu257, Asn258, Thr262, Asp264, Asp266, Ser273, and His275 of CABP4 are essential for binding with the IQ motif. While Mutant-CABP4 was failed to interact properly with IQ motif, which might lead to night blindness. Both complexes were validated with MD simulation; the Wild-type CABP4-IQ complex remained stable at RMSD ranging from 0.4 to 0.5 Å, while the Mutant CABP4-IQ complex showed fluctuating RMSD ranging from 0.2 to 0.8 Å. Residue fluctuations and hydrogen bond analysis highlighted the residues required for interaction of IQ domain with CABP4 for functional rod photoreceptors. Finally, our protocol revealed the role of CABP4 and  $\text{Ca}^{2+}$  in night blindness which could pave the way towards therapeutic intervention against the night blindness.

## Chapter 1

### 1 Introduction

#### 1.1 The Vital Role of Calcium Ions ( $\text{Ca}^{2+}$ ) in the Human Body

Calcium is an essential ion in human cells. It controls the many biological activities in the human body. It is involved in activating enzymes, contracting muscles, and exciting neurons, among other important mechanisms (1). The pathways that regulate the  $\text{Ca}^{2+}$  concentration in the body, including the  $\text{IP}_3$ - $\text{Ca}^{2+}$  pathway, p38-MAPK pathway, the CAM-binding pathway, and other calcium signaling pathways mediated by calcium channels, etc. (2).

#### 1.2 Understanding the Role of $\text{Ca}^{2+}$ Signaling in Cellular Activities

$\text{Ca}^{2+}$  ions play a crucial role as a second messenger in many cellular processes such as cell signaling, neurotransmitter release, enzyme activation and ion channel regulation etc. The release of intercellular  $\text{Ca}^{2+}$  is facilitated through various channels located in the endoplasmic reticulum (ER), such as the inositol 1,4,5-trisphosphate ( $\text{IP}_3$ ) receptors, ryanodine receptors (RyR) and NAADP receptors in lysosomes, and ion channels in mitochondria. These channels are under the regulation of various receptors, triggering a rise in intracellular  $\text{Ca}^{2+}$  concentration (3). The resulting intracellular calcium concentration acts as the initiator of the phosphatidylinositol (PI) calcium signaling pathway, which is important for cell growth. The RyR controls the expression of organogenesis, in cardiac and skeletal muscles (4). The released  $\text{Ca}^{2+}$  from these receptor or calcium channels, binds with calcium-binding proteins that initiated the appropriate mechanism and control the regulatory activity of enzymes. Some of these proteins play a role as calcium buffers and while others serve as essential keys in numerous signaling pathways. Calcium regulates the various upstream kinases and transcription factors although it doesn't directly modulate transcription; instead, it activates specific signaling necessary for transcription processes. In neurons, calcium signals regulate developmental processes, apoptosis, neurotransmitter release, and membrane excitability by voltage-dependent ion channels and plasma membrane receptors (5).

### 1.3 The Impact of Voltage-Gated Calcium Channels (Cav) on Neural Function

The regulation of communication among neurons is controlled by voltage-gated calcium ( $\text{Ca}_v$ ) channels. The calcium-dependent synaptic signaling triggers the release of neurotransmitters from the presynaptic membrane that coordinate cellular activities within the nervous system (6). Voltage gated calcium ( $\text{Ca}_v$ ) channels are classified into high voltage-activated (HVA) and low voltage-activated channels (LVA) that differ in their activation thresholds for calcium current. The low voltage-activated channels are activated below the action potential threshold and while HVA channels are activated after the initiation of the action potential (7).

### 1.4 $\text{Ca}^{2+}$ Channel Diversity and Functionality

Cav1 and Cav2 channels carry high-voltage  $\text{Ca}^{2+}$  current, while Cav3 channels carry low voltage  $\text{Ca}^{2+}$  current. Gene duplication expanded calcium channel diversity: Cav1 split into four L-type (Cav1.1 to Cav1.4), Cav2 into three P/Q or N-type (Cav2.1, Cav2.2, Cav2.3), and Cav3 into three T-type (Cav3.1 to Cav3.3) channels (8). The Cav1 subfamily controlled the biological functions, such as regulation of gene expression, contraction and secretion initiation, synaptic input, and synaptic transmission at ribbon synapses in specialized sensory cells. On the other hand, the Cav2 subfamily plays an important role in initiating synaptic transmission at the fast synapses. The Cav3 subfamily is responsible for controlling the action potential in cardiac myocytes and thalamic neurons (6).

Channel	GENE	CURRENT
Cav1.1 Cav1.2 Cav1.3 Cav1.4	CACNA1S CACNA1C CACNA1D CACNA1F	L-Type
Cav2.1 Cav2.2 Cav2.3	CACNA1A CACNA1B CACNA1E	P/Q-Type N-Type R-Type
Cav3.1 Cav3.2 Cav3.3	CACNA1G CACNA1H CANCA1I	T-Type

Figure 1: Variability in voltage-gated calcium channels at the genetic level (9).

### 1.5 The Functional Domains of the L-type Calcium Channels (LTCCs)

The three main subunits comprising LTCCs are: the pore-forming  $\alpha 1$  subunit, along with auxiliary subunits  $\beta 2$  and  $\alpha 2\delta$  (alpha2-delta). The  $\beta 2$  and  $\alpha 2\delta$  subunits provide a supportive role to the pore-forming  $\alpha 1$  subunit for operating and proteosomal degradation. The  $\alpha 1$  subunit of the LTCCs can be divided into two functional domains based on their topology. The one is the voltage sensor domain and the second is the pore-forming region. The C-terminal of the  $\alpha 1$  subunits acts as a modulatory domain for protein-protein interactions. The C-terminal segments contain, EF hands, pre-IQ, and IQ motif that provides the interaction sites for the apo-CaM. In the retina, CaM-like  $\text{Ca}^{2+}$ -binding proteins (CABPs) regulate the effectiveness of this modulatory mechanism (10).

The  $\text{Ca}_v1.1$  is found in both the skeleton muscle and brain of mammals.  $\text{Ca}_v1.2$  is mainly found in cardiac and smooth muscles, while  $\text{Ca}_v1.3$  is involved in calcium regulation in the heart, smooth muscle, neurons, and endocrine cells. The  $\text{Ca}_v1.4$  channel, on the other hand, is unique to the eyes and immune cells (11).

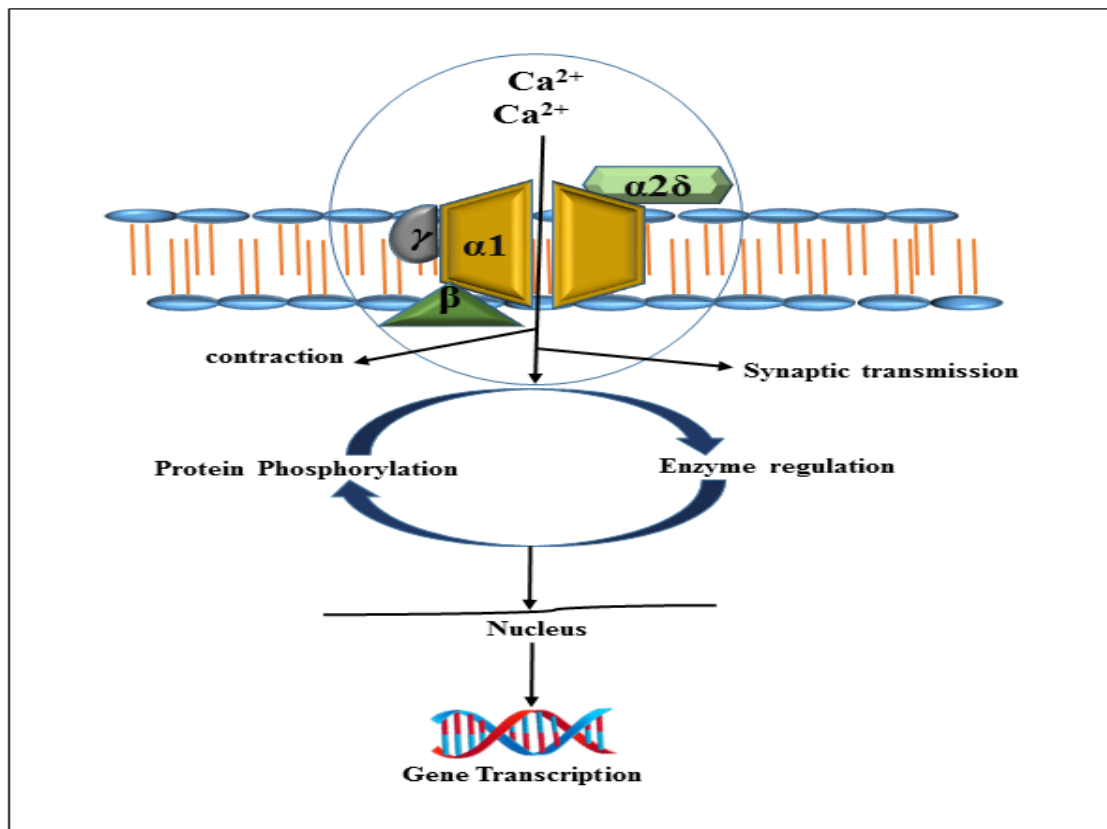


Figure 2. Voltage-gated  $\text{Ca}^{2+}$  channels mediate signal transduction (6).

## 1.6 The Importance of Cav1.4 in Maintaining Normal Transmission of Visual Signals

### Light Conditions

#### **The pre-Synaptic terminal of the rod cell**

In the presence of light, the CNG ion channels are closed. Which results in a decrease in the influx of calcium ions and sodium ions inside the cell (12). The inward dark current is reduced due to ion channel closure, and the membrane gets hyperpolarized. The hyperpolarized membrane potential  $V_m$  is approximately -60mv (13). The change in membrane potential causes the closure of the L-type voltage-gated calcium channel “Cav1.4”. The reduction in calcium ions reduced glutamate release from the presynaptic membrane (14).

#### **The post-Synaptic terminal of bipolar cell**

Due to the closure of Cav1.4, glutamate release from the presynaptic membrane is reduced. In this condition, another neurotransmitter, “GABA” is released from the horizontal cell. It binds to GABA receptors, which are present in the bipolar cell (15). It induced the current in the bipolar cell. The change in bipolar current sends signals to the amacrine cell. After passing signals from amacrine cells to ganglion cells (16). The ganglion cell sends signals to the brain for visual processing.

### Dark conditions

#### **The pre-Synaptic terminal of the rod cell**

In the dark, the CNG ion channels are opened. The influx of calcium ions and sodium ions is increased (17). Due to an increase in the influx of  $Ca^{2+}$ , the amount of  $Ca^{2+}$  in cells is approximately 300–500 nM. The inward dark current increased due to ion channels opening and the membrane getting depolarized. The depolarized membrane potential  $V_m$  is approximately -40mv (13). The change in membrane potential causes the opening of the L-type voltage-gated calcium channel Cav1.4. A large number of calcium ions causes the release of glutamate in higher concentrations from the presynaptic membrane (14).

### The post-Synaptic terminal of bipolar cells

Due to the opening of the calcium channel and the higher release of glutamate from the presynaptic membrane, the glutamate binds to glutamate receptors, which are present at the postsynaptic terminal of the bipolar cell. The binding of glutamate with its receptors changes the membrane potential of the bipolar cell (18). The change in bipolar current sends signals to the amacrine cell which transmits the signal to the ganglion cells (16). The ganglion cell sends signals to the brain for vision, as shown in the Figure 3.

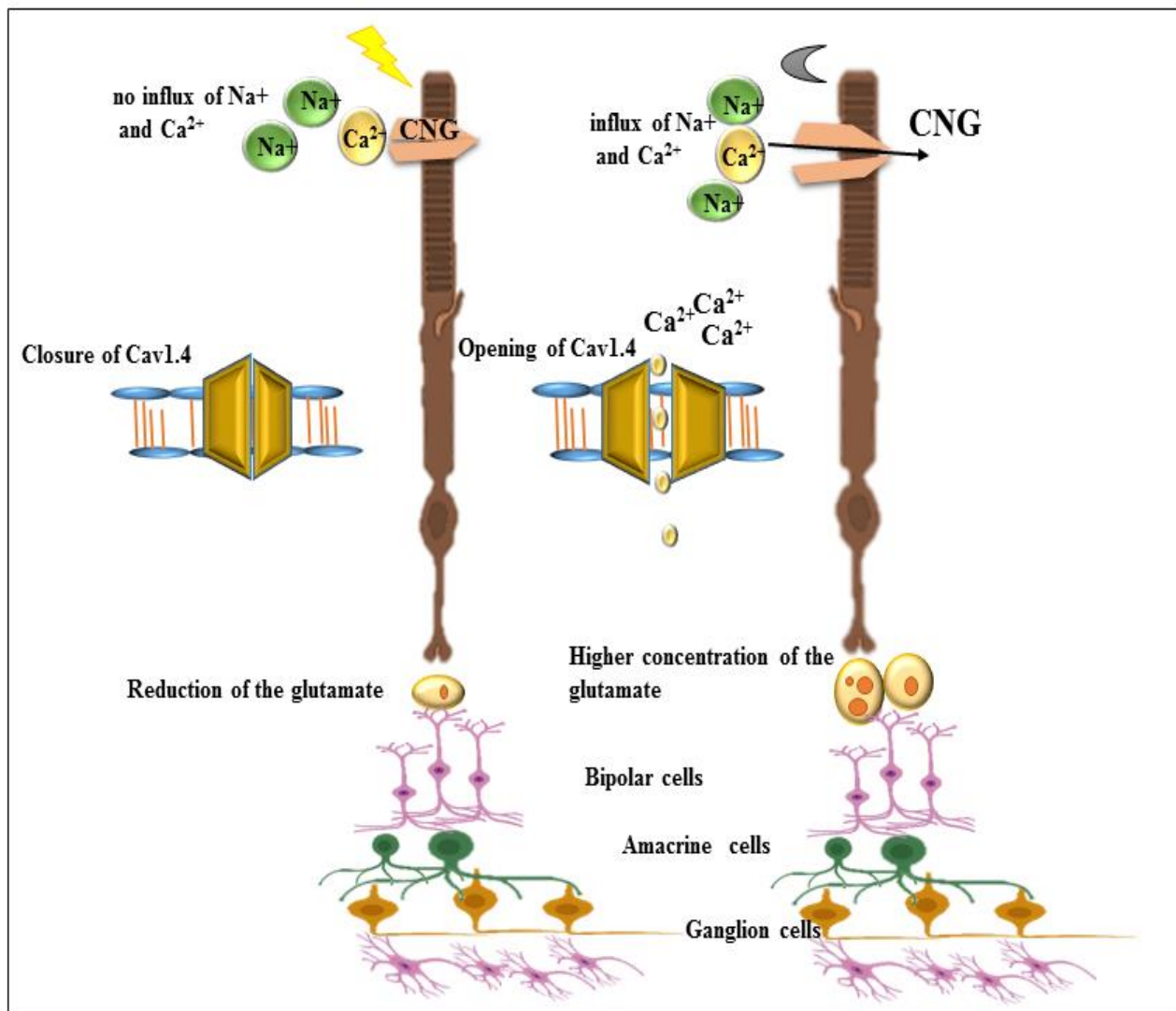


**Figure 3.**Release of glutamate from the presynaptic membrane of rod cell, in dark and light mechanism (14).

## 1.7 The Role of L-Type Calcium Channels in the Pathogenesis of Various Diseases

The different isoforms of the L-type channel play significant physiological functions across various tissues organs, and cells i.e. heart, brain and endocrine cells, etc. Given their diverse functions, LTCCs have emerged as potential therapeutic targets for several human diseases (11). The LTCCs are significantly involved in the neurological system and associated disorders. Blockage of LTCCs in the brain has been shown to provide therapeutic benefits for conditions such as epilepsy and parkinson's disease (19). Cav1.3 play an important role in the excitation of neurons and synaptic plastic in the brain, particularly in response to high concentrations of intracellular calcium influx (20).

The process of cardiac contraction and activation of the myofilaments is regulated by the increased calcium influx by the L-type channel in the heart cycle. Inhibiting Cav1.2 can provide pharmacological benefits in the cardiac vascular system (21). Calcium channel blockers are commonly used to treat hypertension, cardiac ischemia, and arrhythmias (22). Cav1.1 expressed in skeletal muscle tissues and plays a crucial role in regulating muscle contraction. Several diseases are associated with Cav1.1, including paralysis and malignant hyperthermia. It is important to thoroughly investigate and understand these mechanisms to develop effective treatments for these conditions (23). Rod photoreceptors in the retina contain a channel known as Cav1.4 that plays a major role in regulating the influx of  $\text{Ca}^{2+}$  in rod photoreceptors, to control the fusion of synaptic vesicles at the presynaptic membrane. The transmission of visual signals between the rod cell and bipolar cell is strongly dependent on the fusion of synaptic vesicles and the release of neurotransmitters from the presynaptic membrane of the rod cell. However, the mutation in the gene that translates the channel protein can lead to reduced  $\text{Ca}^{2+}$  influx and altered channel gating properties, resulting in decreased channel activity. Patients with such mutations, often experience night blindness issues with myopia and low visual acuity (14).

## 1.8 The Disease Associated with Cav1.4 in the Transmission of Visual Signals

In the dark mechanism,  $\text{Ca}^{2+}$  ions concentration in the cell is higher due to the opening of the CNG ions channel. Due to this, membrane potential gets depolarized in the absence of light (14).

However, in certain disease conditions, such as congenital stationary night blindness, the L-type voltage-gated calcium channel Cav1.4 fails to detect changes in the membrane potential and remains closed. The result is higher  $\text{Ca}^{2+}$  ions concentration in the rod cells is due to the malfunctioning calcium-binding protein in the cell which is CABP4 (calcium-binding protein 4). As a result, the membrane potential is further depolarized (24). This affects photoreceptor signal processing and directly impacts signal transmission from rod photoreceptors to retinal bipolar cells. The closure of the  $\text{Ca}^{2+}$  channel does not trigger the glutamate release from the presynaptic membrane in a disease condition. In this situation, no signals are transmitted to the brain for visual processing in a dark situation. The result of this situation is that vision at night become difficult. The condition refers to night blindness, as shown in Figure 4 (25). The main symptoms of the disease condition are poor vision in the dark or a delay in dark adaptation at night. The severe condition may result in myopia or hyperopia.

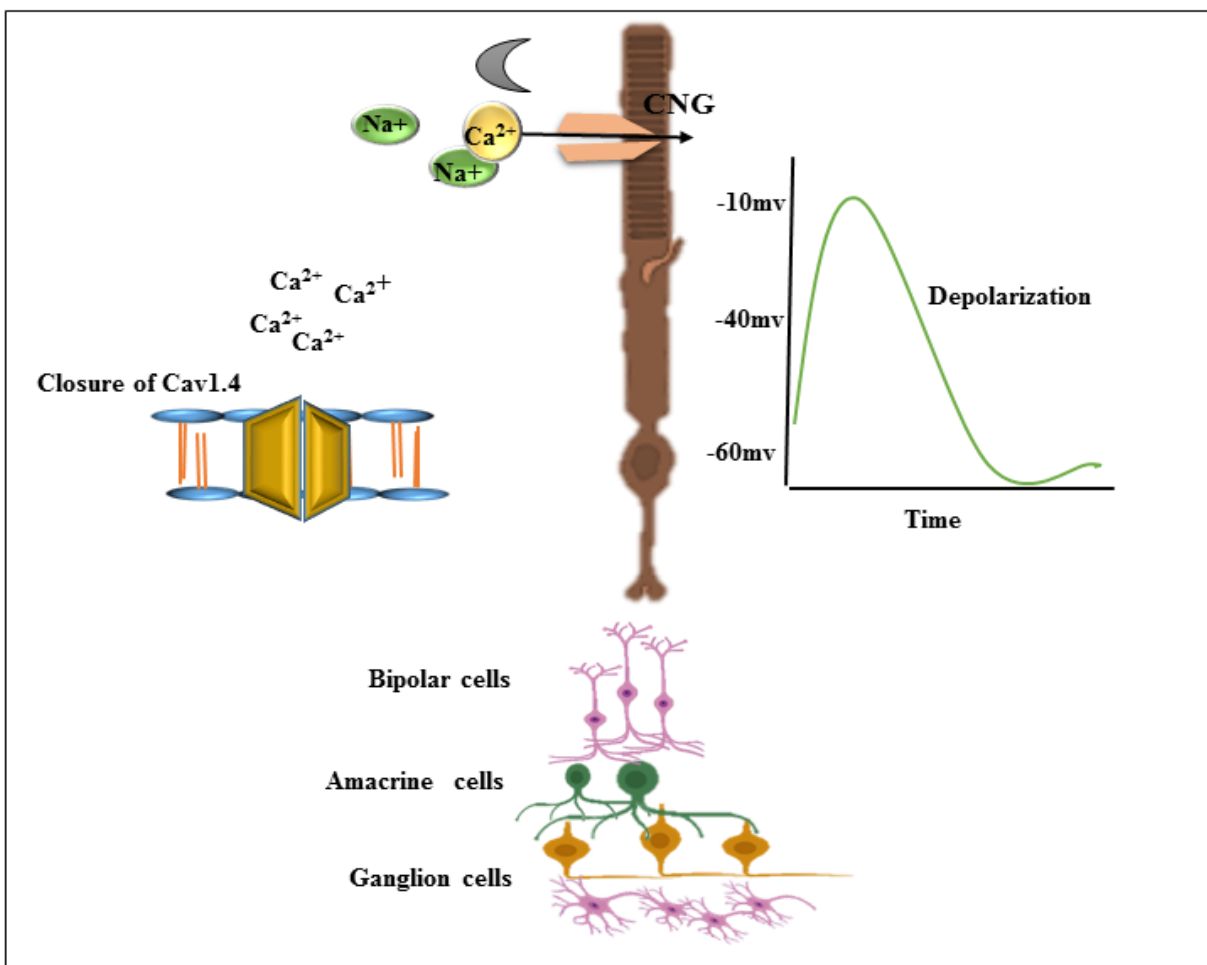


Figure 4. The role of Cav1.4 channel closure in inhibiting signal transmission (25).



## 1.9 Therapeutic Options for Retinal Diseases

Various approaches can effectively treat retinal diseases, including Retinitis Pigmentosa, myopia, and night blindness.

### 1.9.1 Spliceosome-mediated RNA *trans*-splicing (SMaRT)

Trans-splicing is a type of splicing reaction that occurs in premature mRNA molecules. In which two exons are joined together. This process is found in different organisms including trypanosomes, rats, and humans that use the cell's spliceosome machinery. Researchers have developed a novel approach to address mutations that impair protein function. This approach involves the use of a pre-mRNA trans-splicing molecule (PTM). It consists of three key components. The first is a binding domain that specifically targets the endogenous pre-mRNA molecule. The second is artificial introns and the third and most critical component is the coding domain, which replaced the mutated portion of the pre-mRNA with the functional coding domain. This approach allows for the replacement of the mutated part of the mRNA with the functional coding domain at the transcriptional level. Once the mature mRNA is produced, the normal functional protein can be translated, thereby restoring the functionality of the gene. This technique has the potential to be an effective therapeutic approach for genetic diseases caused by mutations that impair protein function (26).

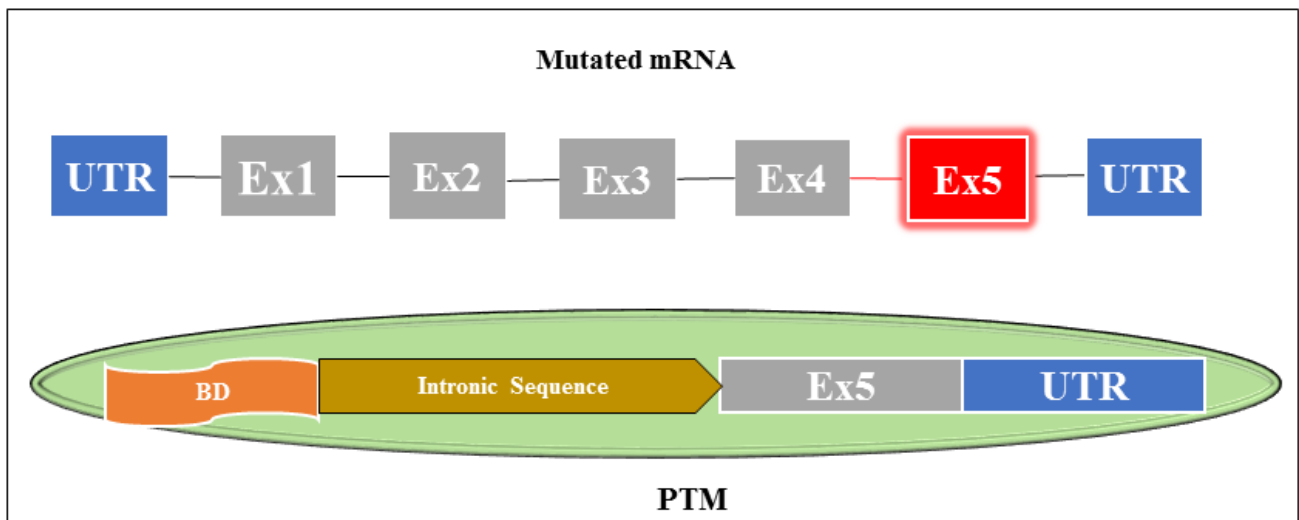


Figure 5. PTM design for the treatment of Retinal diseases (26).

## 1.9.2 Gene Therapy

Gene therapy is a method of treating genetic disorders by targeting the disease at the DNA level. This technique uses the host's machinery to construct the foreign DNA to replace the mutated DNA. The requirements for gene therapy are a promoter that is important for gene transcription, a vector that facilitates DNA delivery to specific cells, and the host machinery that is used to construct the mutated DNA. Once the mutated DNA is replaced with functional DNA, normal gene expression occurs, which is essential for protein translation (27).

## 1.10 Problem Statement

The Mutant-CABP4 protein subsequently gets misfolded and thus, changes in its conformation hamper binding with the IQ motif of Cav1.4 for normal photo mechanism, as shown in the Figure 6 (28). The results show that the ICDI auto-inhibitory domain of the channel becomes activated and binds with the IQ motif. As a result, the channel becomes inactive in the absence of light, and no signals are transmitted to the brain for visual processing (29). Therefore, validation of CABP4 as a potential drug target and a comparison of conformations changes of wild type and Mutant-CABP4 could pave the way towards a potential therapeutic intervention against night blindness.

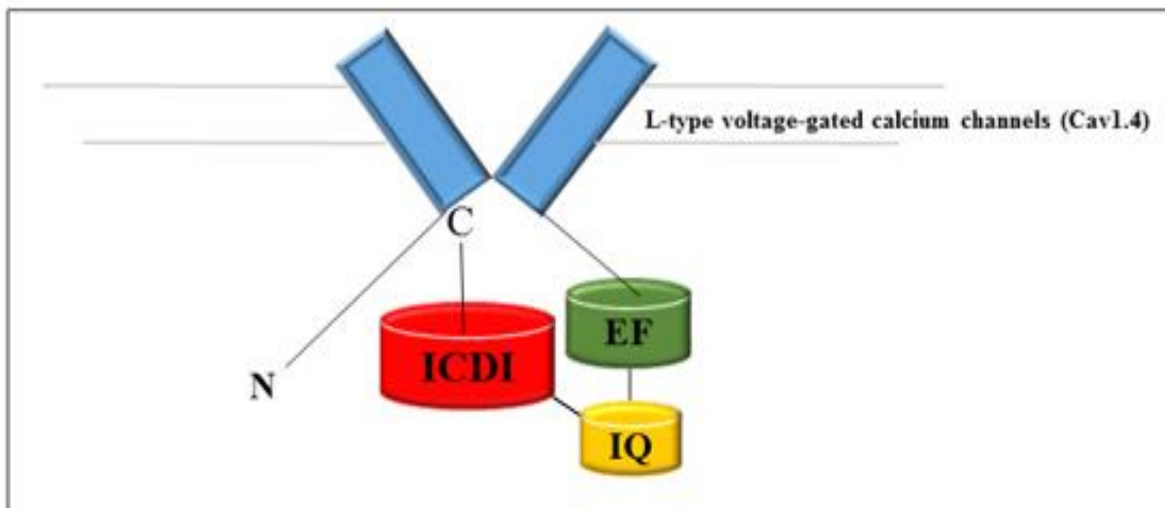


**Figure 6. Illustration of ICDI-mediated closure of  $\text{Ca}^{2+}$ -dependent channel Cav1.4 (29).**

### 1.11 Objectives

- To probe the regulatory mechanistic of CABP4 in day and night conditions
- To design a BRN (Biological Regulatory Network) and perform dynamic simulation of  $\text{Ca}^{2+}$  and CABP4 pathway for the regulation of visual signaling under normal and disease conditions.
- To probe the binding hypothesis of CABP4

## Chapter 2

## 2 Literature Review

### 2.1 Target Validation of CABP4: A Promising Approach for Night Blindness Treatment

CABP4 belongs to the family of calcium-binding proteins and is present in the synaptic terminal of photoreceptor cells. It interacts with L-type calcium channel Cav1.4, plays a significant role in regulating calcium influx and controlled the release of neurotransmitters from synaptic terminals to bipolar cells in a normal functioning visual system. Mutations in the CABP4 have been linked to several diseases, such as congenital stationary night blindness, rod-cone dystrophy, and retinal degeneration (28).

### 2.2 Rod-Cone Dystrophy

It is an inherited retinal disease characterized by the progressive degeneration of the rod and cone photoreceptors. This degeneration often results in night blindness, followed by a gradual reduction in the visual field. CABP4 is a gene that has been associated with autosomal recessive rod-cone dystrophy. Mutations in this gene can result in dysfunctional calcium signaling in photoreceptor cells, which in turn can lead to impaired neurotransmitter release between the synaptic terminal and bipolar cells in the retina. This disruption in the signaling pathway can ultimately lead to the degeneration of both rod and cone photoreceptor cells and the development of rod-cone dystrophy (30, 31).

The discovery of the novel mutation p.Arg216X in CABP4 through wet lab approaches provides strong support for targeting the CABP4 in Rod-cone dystrophy disease. This mutation causes a loss of functionality in photoreceptors. Gene analysis of this mutation shows that patients with the disease have a homozygous c.646C>T substitution in exon 4 that replaces arginine with a stop codon. This mutation causes changes in the structure of CABP4 that affect the functionality of the protein. The mutant CABP4 loses the two calcium-binding EF domains from its structure, which impairs its ability to function properly (32).

This disease condition is called rod-cone dystrophy, which is characterized by a reduction in visual acuity, nystagmus, photophobia, and severely abnormal color vision. Therefore, a better understanding of the role of CABP4 in the pathogenesis of rod-cone dystrophy may aid in the discovery of possible therapeutic targets for this condition (33).

### 2.3 Congenital Stationary Night Blindness(CSNB)

CSNB is characterized by a reduced ability to see in low light conditions and night blindness, which are key symptoms of this retinal disorder. Mutations in several genes including NYX, CACNA1F, CABP4, GRKI, GRM6, TRM1, and RHO have been linked to the development of CSNB. The electroretinogram (ERG) is a diagnostic tool used to differentiate between two types of CSNB. In CSNB type 1 (CSNB1), the function of the rod pathway is completely absent, while in CSNB type 2 (CSNB2), both the rod and cone pathways are impaired. The impaired signaling cascade in (CSNB2) is characterized by a major mutation in CABP4 and CACNA1F genes (28, 34).

The two different mutations in the CABP4 gene, (c.800\_801delAG and c.370C→T), reduce the transcript levels by 30 % - 40 % and result in the translation of the nonfunctional protein. This reduction in CABP4 levels leads to signaling defects in individuals with these mutations, ultimately causing the development of conditions such as congenital stationary night blindness type 2 (CSNB2) (28). Mutation screening and gene expression analysis of the c.800\_801delAG, mutation in the CABP4 have revealed alterations in splicing sites. This mutation has also been found to cause a translational frameshift mutation p.Glu267fs, which leads to the addition of 91 amino acid residues and alters the protein structure. Novel amino acids can modify the function of the EF<sub>4</sub>, Ca<sup>2+</sup> binding domain in CABP4. This change can affect the protein's ability to bind to calcium ions, decreasing its binding affinity and capacity. Consequently, the modified protein may not be able to regulate the activity of the L-type calcium channel effectively, leading to impaired signaling to bipolar cells and ultimately affecting normal vision (35).

The substitution mutation in exon 2, c.370C→T, causes an amino acid change from p.Arg124Cys. This mutation results in a reduced level of transcripts and translation of a limited amount of functional protein. While this situation does not entirely block signaling, it can lead to a condition known as CSNB2 (32).As such, targeting CABP4 may hold promise as a potential therapeutic strategy for treating vision disorders associated with impaired calcium signaling in

photoreceptor cells. Further research is needed to better understand the mechanisms underlying these conditions and to develop effective treatments that can help restore normal visual function.

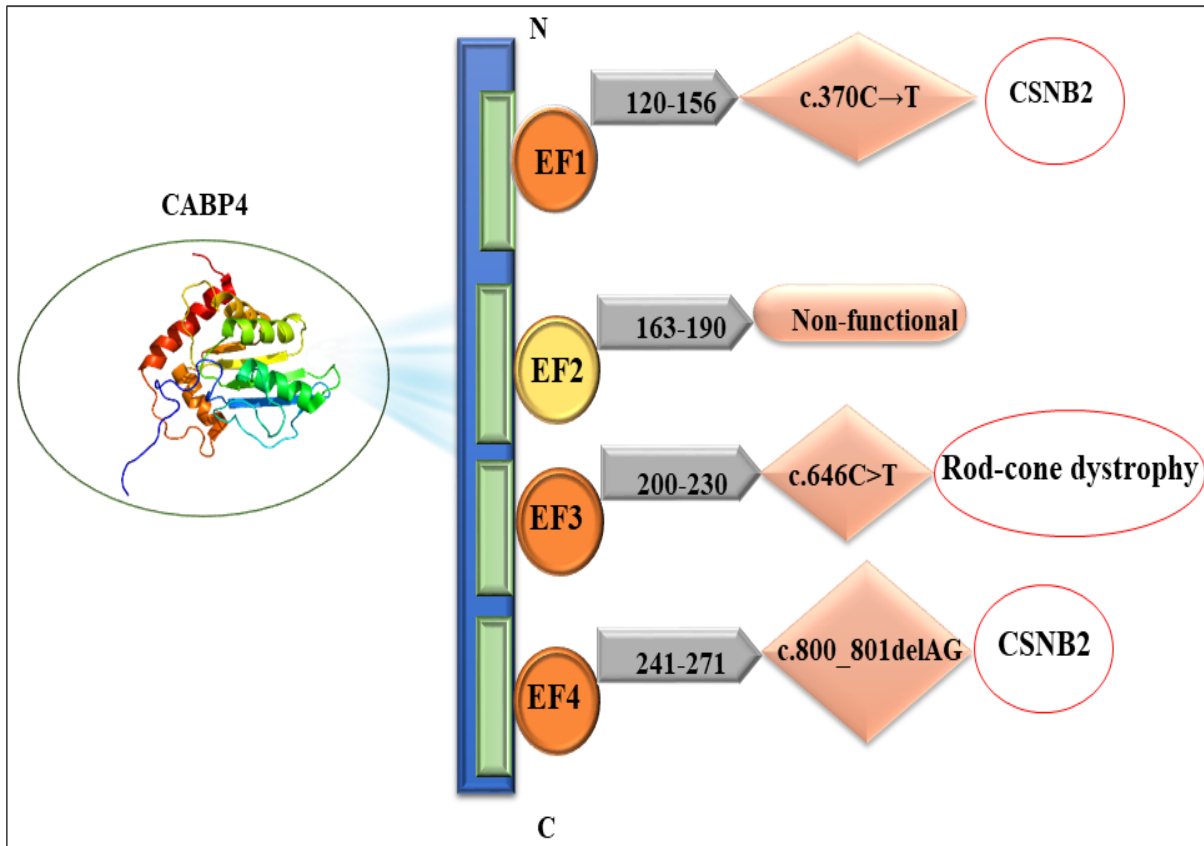
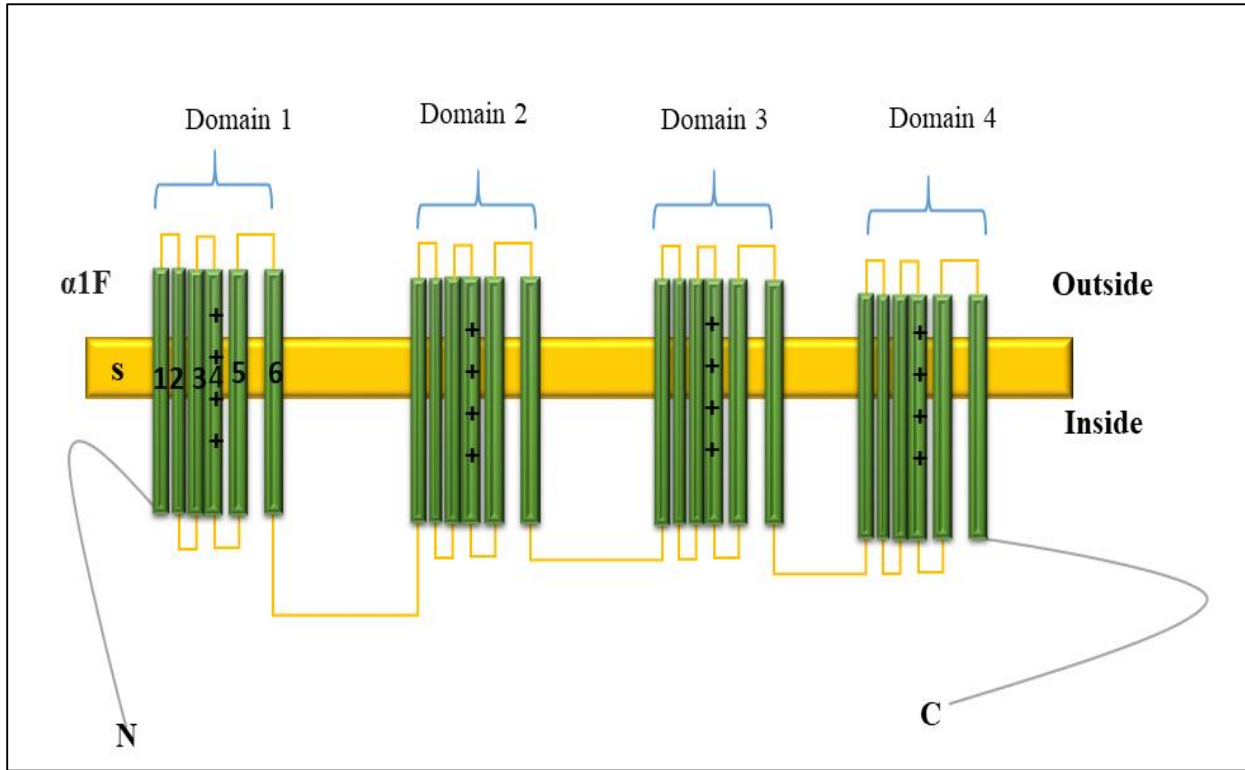


Figure 7. Disease associations within the calcium domain of CABP4 (28, 32, 35).

## 2.4 Functional Subunits of Cav1.4

The Cav1.4 channel is an L-type voltage-gated channel (VGCC) situated in the presynaptic terminal area of photoreceptors. It is formed through the expression of the CACNA1F gene, which comprises 48 exons responsible for encoding the  $\alpha$ 1F subunit protein. This protein spans 1997 amino acids and plays a crucial role in defining the characteristics of the alpha 1F subunit of the voltage-gated channel. Within this subunit, there are four homologous domains positioned between the N and C termini. Each of these domains contains six transmembrane alpha helix segments (S1–S6) (11, 36). The domain formed by S1-S4 segments serves as the voltage sensing unit, detecting voltage changes. In contrast, the S5-S6 segments are in charge of controlling the opening and closing of the channel. The  $\alpha$ 1 subunits define the VGCC channel, with  $\alpha$ 1F being specific to the

Cav channel. Additional subunits contributing to the characterization of Cav channels encompass  $\beta$ ,  $\alpha 2\delta$ , and Y subunits (37).



**Figure 8: Structure of  $\alpha 1F$  subunit of Cav1.4 (38).**

The alteration in the CACNA1F gene results in retinal irregularities in humans. The presence of a missense mutation within this gene leads to reduced  $\text{Ca}^{2+}$  influx and alters the channel gating properties, preventing the channel from maintaining an active state. As a consequence of the mutated CACNA1F gene, there is a disruption in photoreceptor synaptic transmission. This genetic mutation interferes with the normal visual pathways within the retina and hinders the functionality of second-order neurons. Among the effects of this mutation, the most significant clinical manifestation is observed in the form of congenital stationary night blindness type 2. Individuals affected by CSNB2A experience challenges with night vision, along with myopia and diminished visual acuity (39).

The  $\beta 2$  and  $\alpha 2\delta$  subunits have significant involvement in modulating the gating characteristics of the Cav1.4 channel. A genetic mutation within the  $\beta 2$  subunit gene induces alterations in the channel's responsiveness. The  $\alpha 2\delta$  subunits are coded by the CACNA2D1 gene and are responsible for regulating the release of glutamate from the presynaptic membrane. The presence of a mutation in the CACNA2D1 gene results in decreased protein expression. This

genetic anomaly disrupts the normal regulation and leads to visual impairments in humans, ultimately giving rise to the condition known as cone dystrophy (40).

## 2.5 The Impact of CABP4 on Channel Activation Voltage

In photoreceptors, the opening of CNG channels in the absence of light causes an influx of calcium ions into the cells, resulting in the depolarization of the membrane and the opening of Cav1.4 channels. The C-terminal region of Cav1.4 contains the EF-hands domain, pre-IQ and/or IQ domains, and important functional region C-terminal modulator ICDI/CTM. The IQ domains are important for the interaction of calcium-binding proteins. The lack of calcium-dependent inactivation (CDI) in Cav1.4, distinguishes it from other L-type voltage-gated calcium channels, making it activate at more negative voltages and exhibit slow inactivation (14).

CABP4 (calcium-binding protein 4) that regulates the voltage-gated calcium channels in the retina. It is structurally similar to CaM and interacts with the IQ domain of Cav1.4, changing the activation curve towards more negative values. This interaction disrupts the binding of ICDI/CTM with Cav1.4 domains, leading to the activation of the channel in the dark. Certain residues in CABP4, including Phe137, Glu168, Leu207, Ile209, Met251, Phe264, and Leu268, are crucial for their interaction with the IQ domain of Cav1.4. In the absence of CABP4, the reduction of calcium influx and voltage lead to a decrease in the transmission of visual signals to the brain, resulting in night blindness (29).

The Cav 1.4 channels operate at more negative potential. The absence of CABP4 cause, the reduction of  $\text{Ca}^{2+}$  influx and the reduction in the voltage of about 50% in rod photoreceptor that cannot regulate the activity of Cav1.4 in the dark (35). Mutations in CABP4 do not negatively affect the voltage-dependent activation of Cav1.4, but they do bind to the channel and do not antagonize the ICDI domain. This change in the window current and the approach of CaM to the effector site of the channel keep Cav1.4 channels closed in the dark, preventing the transmission of visual signals to the brain (41).



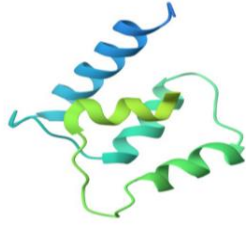
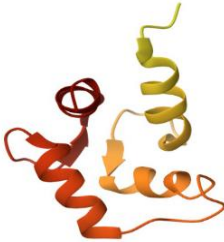

## 2.6 Structural Dynamics of CABP4 and Cav1.4 IQ-Motif Domain

CABP4 is a protein that is present in the retina and is responsible for modulating the activity of L-type voltage-gated calcium channels, specifically Cav1.4 channels in rod cells. The protein has two distinct regions, known as the N-lobe and the C-lobe. The C-lobe consists of EF3 and EF4, which are capable of binding to calcium ions, while the N-lobe consists of EF1 and EF2. EF1 can bind to either calcium or magnesium ions, while EF2 is nonfunctional (28, 42). The N-terminal region of CABP4, consisting of the first 99 residues, is considered to be unstructured based on limited proteolysis studies. Removal of this region has been shown to increase the protein's solubility without affecting its ability to bind to calcium ions or its target sites. An NMR structure is available for CABP4 (residues 100-271), which was experimentally obtained by deleting the N-terminal region. The protein can be divided into three distinct regions: CABP4(1-100), which consists of the N-terminal region; the N-lobe (residues 100-200); and the C-lobe (residues 198-271) (29).

In the mechanism of light activation of the photoreceptors, CABP4 binds with  $Mg^{2+}$ . This binding is due to the lower calcium concentration in the cell. Conversely, in the absence of light (dark conditions), CABP4 becomes active due to the higher calcium concentration in the cell. It then regulates the activity of the Cav1.4 channel, which transmits signals to the brain for normal visual processing (43).

The NMR structure of CABP4 (100-271) was determined by separately calculating the structures for the N-lobe and C-lobe (44). To validate these structures, PRO-CHECK analysis was performed. The results showed that 82% of the residues in the N-domain and 74.2% of the residues in the C-domain were located in the favorable region of the Ramachandran plot. The N-lobe of CABP4 has hydrophobic residues (Leu122, Leu150, and Met164) on its surface, whereas the hydrophobic residues of C-lobe (Leu207, Phe214, Ile222, Leu235, Leu239, Met251, Phe264, and Leu268) interact with the IQ motif (residues 1579–1605) of Cav1.4. The helical structure of the IQ motif of Cav1.4 is derived from the previously known crystal structure of Cav1.2 (29).

**Table 1: The PDB IDs and structures of the CABP4 and IQ motif.**

Protein	PDB-ID	Structure	Reference
CABP4-N lobe	2M29		(29)
CABP4-C lobe	2M28		(29)
IQ motif	2BE6		(29, 45)

## 2.7 Interaction between CABP4 and IQ-Motif

The current literature reveals that the structural conformation of the IQ motif in Cav1.4 remains indefinable, leading to the utilization of the Cav1.2 structure as a reference for constructing a homology model of the Cav1.4 IQ motif (46). This modeling strategy is aimed at uncovering the interaction dynamics between the IQ motif and CaBP4 in rod photoreceptors. Employing the HADDOCK online server, docking was independently carried out for both the N and C lobes of CaBP4. The investigation pinpointed specific residues namely Glu121, Leu122, Gly123, Phe137, Met154, Phe186, Thr198, Ala199, Leu207, Phe214, Leu235, Gly236, Met251, Glu263, Phe264, and Leu268 as active participants in the interaction within the HADDOCK docking framework.

Subsequently, an ensemble of docked structures was generated and analyzed, with the ultimate selection of the most favorable structure driven by the criterion of the lowest RMSD value.

Findings from this inquiry expose that both the C and N lobes of CaBP4 establish connections with the IQ motif. Notably, specific residues within the IQ helix engage in hydrophobic interactions with their counterparts in the CaBP4 C-lobe. Interestingly, mutations at residue 1595 (Y1595E) on the IQ helix led to a reduction in interaction strength. Analogously, mutations at residues 251, 264, and 268 (M251A, F264E, L268A) on CaBP4 also weakened interaction potency(24). Furthermore, a comparative analysis highlighted a significant structural correspondence between the main chain configurations of the C-lobes of CaBP4 and CaM in both complexes, with an RMSD value of 1.5 Å (46).

Specifically, the N-lobe of CaBP4 engaged in a hydrophobic interaction with the IQ-helix. This interaction was highlighted by the interaction between CaBP4's Phe137 and the IQ helix's Phe1586. Additionally, an electrostatic interaction materialized between CaBP4's Glu168 and the IQ helix's Arg1597. Interestingly, the interaction between the IQ helix and the N-lobe of CaBP4 showed a different orientation when compared to the IQ helix's interaction with the CaM N-lobe (45). This contrasting location seems to contribute to the heightened binding affinity of calcium L-type channels.

In conclusion, the docking interaction involving the IQ motif and both lobes of CaBP4 showcases resemblances to the CaM binding with the Cav1.2 IQ. These parallels provide support to the hypothesis that CaBP4's mechanism involves hindering calcium-dependent inactivation and competing with CaM for binding to the IQ motif of Cav1.4. This mechanistic insight offers valuable understanding into how Cav1.4 channels stain open in dark-adapted rod photoreceptors, particularly under conditions of higher intracellular  $\text{Ca}^{2+}$  concentrations (29).

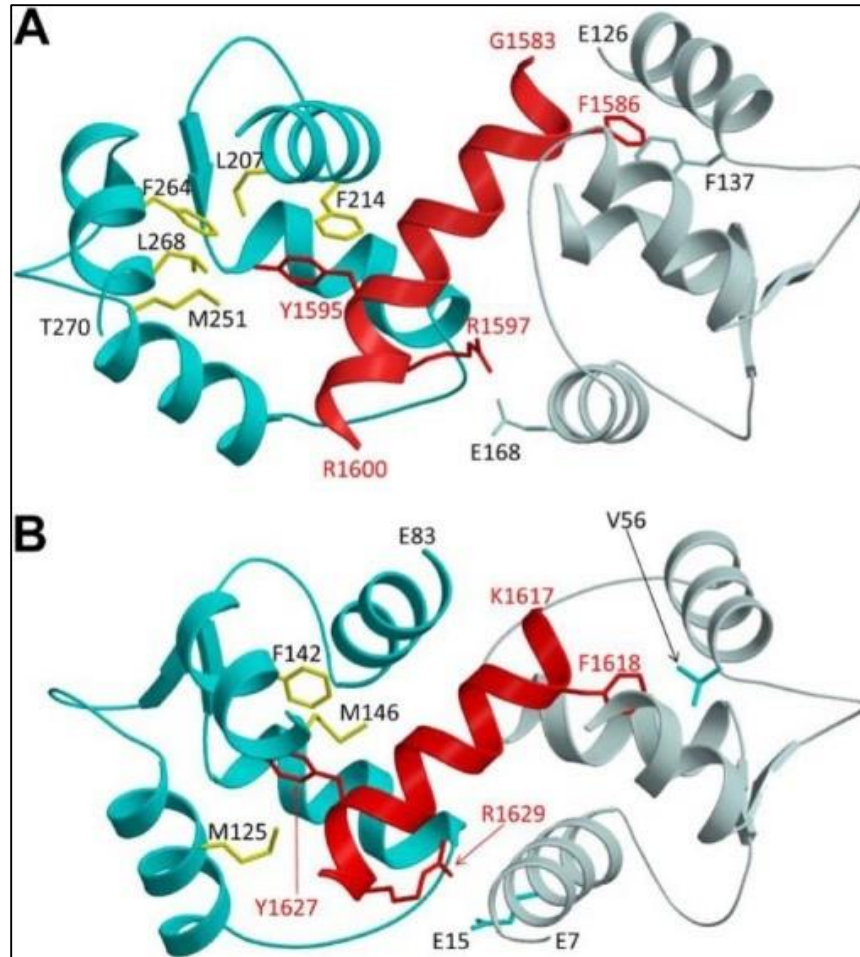


**Figure 9:** CaBP4 bound to IQ Motif, in this model, the N-lobe is depicted in a light gray shade, the C-lobe is highlighted in cyan color, and the IQ helix is distinguished by its red color (29).

## 2.8 Emerging Therapeutic Approaches for Retinal Treatment:

Gene and RNA-based therapies have shown promising results in the treatment of inherited retinal diseases. The treatment options for retinal diseases vary based on the specific type and severity of the condition. Here are some commonly utilized therapies for retinal diseases:

**Gene-Based Therapies** Gene augmentation is a type of gene therapy that aims to replace a faulty gene with a functional gene using vector transporters. By introducing the corrected gene into the affected cells, this therapy enables the production of therapeutic proteins within the eye, essentially creating an ocular bio-factory. This approach has shown promising results in the treatment of inherited retinal diseases, allowing for the restoration or improvement of the function of affected retinal cells (47).

Another approach is gene editing with Clustered Regularly Interspaced Short Palindromic Repeats Technology (CRISPR), which can help treat certain eye diseases. Scientists use different types of bacterial nucleases, such as Cas9 from *Streptococcus pyogenes* or *Campylobacter jejuni*, along with CRISPR, to perform gene editing. They often deliver these gene editing tools using viral vectors like AAV and lentivirus, although some researchers have also tried delivering pre-assembled Cas9 ribonucleoproteins directly to reduce immune and antibody responses.

The gene editing tools are injected into the eye, either under the retina or into the vitreous gel. They target genes responsible for producing certain proteins like VEGF receptor 2 (VEGFR2), VEGF-A, and hypoxia-inducing factor-1 $\alpha$  (HIF-1 $\alpha$ ), which play a role in promoting blood vessel growth. The aim is to edit these genes and suppress abnormal blood vessel growth for an extended period (48). However, there is a risk of unintended effects from gene editing, such as mutations occurring in other parts of the genome. Scientists are mindful of this risk and work to minimize it. Clinical trials involving humans are expected in the future to evaluate the effectiveness and safety of these gene editing techniques for endovascular AMD and other eye diseases.

RNA-based therapies, such as Post-Transcriptional Gene Silencing, have emerged as effective strategies for treating retinal disorders. One prominent RNA-based approach is RNA interference (RNAi), which utilizes small RNA molecules, including short interfering RNA (siRNA), short hairpin RNA (shRNA), or microRNA (miRNA), to bind to and degrade messenger RNA (mRNA). This process effectively silences the expression of targeted genes involved in the retinal disease. RNAi-based therapies have shown promise in preclinical and clinical trials for the treatment of retinal disorders, offering a potential avenue for therapeutic intervention (49).

## **2.9 Spliceosome-mediated RNA trans-splicing (SMaRT)**

Trans-splicing is a type of splicing reaction that occurs in premature mRNA molecules. In which two exons are joined together. This process is found in different organisms including trypanosomes, rats, and humans, that use the cell's spliceosome machinery. Researchers have developed a novel approach to address mutations that impair protein function. This approach involves the use of a pre-mRNA trans-splicing molecule (PTM). It consists of three key components. The first is a binding domain that specifically targets the endogenous pre-mRNA molecule. The second is artificial introns and the third and most critical component is the coding domain, which replaced the mutated portion of the pre-mRNA with the functional coding

domain. This approach allows for the replacement of the mutated part of the mRNA with the functional coding domain at the transcriptional level. Once the mature mRNA is produced, the normal functional protein can be translated, thereby restoring the functionality of the gene. This technique has the potential to be an effective therapeutic approach for genetic diseases caused by mutations that impair protein function (26).

## Chapter 3

### 3 Methodology

#### 3.1 Biological Regulatory Network (BRN) Construction and its Dynamic Simulation

The three BRN (Biological Regulatory Network) was constructed using existing literature and (Kyoto Encyclopedia of Genes and Genomes) KEGG pathways(50). yEd software was employed to establish protein-protein interactions within the light-activated BRN, low-light conditions/dark response BRN, and night blindness visual response BRN. The primary focus of the light BRN was to examine different light responses concerning  $\text{Ca}^{2+}$  levels, CABP4 concentrations, and their corresponding effects on visual signaling and feedback mechanism in light conditions. The main objective of the dark BRN was to investigate the behavior of  $\text{Ca}^{2+}$  and CABP4 at various concentrations in the context of visual signaling under low-light conditions. In the case of night blindness/disease, the BRN was constructed to explore the impact of CABP4 concentration on visual responses in the presence of  $\text{Ca}^{2+}$  concentration.

To build a discrete biological regulatory network model, the Java Genetic Regulatory Network Simulation Framework (Jimena) was employed (51). The model assigned specific values to each item in the network: 0.0 indicated no response in BRN, 0.5 denoted moderate active, and 1.0 represented hyperactive in the Biological Regulatory Network. The responses of  $\text{Ca}^{2+}$  and CABP4 were observed under different conditions for visual signaling. Jimena was used to extrapolate the various peaks of  $\text{Ca}^{2+}$  signaling in visual signaling and the feedback mechanism. The network's dynamic behavior was studied by simulating it using the **SQUAD** simulation technique. SQUAD is an algorithm that relies on binary decision diagrams. By treating the network as a discrete dynamic system, the SQUAD approach generates a continuous dynamical biological regulatory network by identifying the stable states of the network (52). The model of BRN was designed using normalized Hill functions. With the SQUAD decay set to 1.0 and SQUAD steepness set to 10, and a step size of 0.05, the network was simulated for 50 seconds of simulation time. This simulation aimed to investigate the dynamic behavior of the selected entities,  $\text{Ca}^{2+}$  and CABP4, within the regulatory network.

### 3.2 Data Collection

The structural data for the target protein *Human-CABP4*, associated with night blindness, was not available in the RCSB Protein Data Bank. Thus, obtained from the ALPHA fold (53), and the corresponding PDB files were downloaded. To ensure protein structure stability, a 100ns simulation was performed to determine the most stable conformation of the protein structure. However, the 3D structural availability of the *Mutant-CABP4* was not available. To address this limitation, mutant residues were manually added into the wild type and a homology model was built using MODELLER (54). A 200ns simulation was then conducted to identify the best stable conformation of the protein structure.

For the design of the 3D structure of the receptor region of Cav1.4 (IQ motif), MODELLER was utilized. The following steps were followed to identify the template for the Cav1.4 (IQ motif). The **IQ** motif region (Human-Cav1.4) was searched using a Motif Finder tool. The identified region was subjected to a BLAST search to find the best template, which was the Human Cav1.2 regions (PDB id - 3G43). The E and F chains of Human Cav1.2 were used for homology modeling with MODELLER. The resulting homology model was validated using a Ramachandran plot. By following these methods, the structural data of the *Mutant-CABP4* and Cav1.4 IQ motif were obtained and validated for further analysis.

### 3.3 Molecular Docking

To investigate the molecular interaction between Wild CABP4 and its receptor, and Mutant CABP4 and its receptor, a rigid protein docking approach was performed using HADDOCK (55). The docking process involved these computational steps within the server:

- Active and passive residues: were defined for each molecule, with active residues contributing to binding interactions and passive residues contributing to the overall structure.
- RMSD clustering: The resulting docking structures were subjected to RMSD clustering to identify similar conformations.
- Structure refinement: A refinement step was performed on the selected structures to optimize their quality and accuracy.

Following the above steps, top-ranked docking structure was selected based on its relatively low energy and z-score. Through these steps, the molecular interaction between CABP4 and its



receptor was explored using rigid protein docking with HADDOCK(56). The selected docking structure provides insights into the potential binding mode and interaction between the two proteins.

### **3.4 Analysis and Visualization of Docked Complexes**

Final docked complexes were analyzed to investigate the interaction between protein residues within the docked complex. The interaction between residues, including information about bonded and non-bonded contacts, was determined using the PDBsum online server (40). The visualization of all interacting residues was done by using the pymol software (57).

### **3.5 Molecular Dynamic Simulation of the Docking Complexes**

The stability of the docked complexes comprising Wild-type CABP4 with IQ motif and Mutant CABP4 with IQ motif was assessed using molecular dynamics (MD) simulations. To ensure the reliability of the docked complex binding residues and hydrogen bonds, the GROMACS 2019.6 software was used for the molecular dynamics simulations (58). The docked complex structures were generated using the OPLS force field. Solvation was performed in a periodic box utilizing the SPC216 water model, and the resulting systems were neutralized by adding Na<sup>+</sup> and Cl<sup>-</sup> ions. To eliminate steric clashes within the complexes, initial energy minimization was carried out employing the steepest descent minimization algorithm, with 5000 steps and a tolerance of 1000 J/A. Subsequently, under constant temperature and pressure conditions, we reached an equilibrium state of minimum energy for a pressure of 1000 ps. To maintain a constant temperature of 300K and pressure of 1 atm throughout the MD simulation sessions, the Berendsen thermostat and barostat were employed. MD runs were performed, each with a duration of up to 100 ns, to thoroughly investigate the behavior of the docked complexes over extended periods.

## Chapter 4

### 4 Results

#### 4.1 Biological Regulatory Network (BRN) Construction of Light Visual Cascade:

The activators and inhibitors that interact with  $\text{Ca}^{2+}$  and CABP4 were selected from BRN. The visual signaling and no visual signaling responses were selected as two outcomes in the results of the simulation. It was found that Rhodopsin serves as a downstream signaling target of  $\text{Ca}^{2+}$ , as its activation also leads to the activation of Transducin (59), which plays a major role in visual signaling. Further, Transducin activates the GC, which is considered the most critical factor in controlling visual processing. The activity of CNG ion channels is modulated by the GC, leading to a negative regulation of intracellular  $\text{Ca}^{2+}$  levels. Closure of the CNG channels results in a decrease in intracellular  $\text{Ca}^{2+}$  concentration, leading to membrane hyperpolarization. This alteration in membrane current initiates subsequent signaling to the brain, facilitating visual processing under illuminated conditions. Generally, the calcium-binding protein CABP4 remains inactive in response to light stimuli. Generally,  $\text{Ca}^{2+}$  acts as a down-regulator of CABP4 and Recoverin, as lower concentrations of  $\text{Ca}^{2+}$  during light responses play a role in controlling visual processing, as shown in the Figure 10. Another important component is Rhodopsin kinase, which downregulates Rhodopsin but activates Arrestin (60). Arrestin is also a significant factor in the BRN as it controls the feedback mechanism associated with non-visual signaling or light recovery responses (61).

The network was initialized with all nodes having a concentration value of (0.0), inactive state. The light was considered the initiator of the network. Continuous modeling through dynamic simulations was employed to study the behavior of the network. Concentration levels in the BRN were categorized as follows: The inactive state was represented by a concentration level of 0.0. Lower inactivation states were denoted by concentration values ranging from 0.1 to 0.4. The active state was represented by concentration values between 0.5 and 0.9. The hyperactive state was represented by a concentration value of 1.0. The activation and inhibition relationships between the nodes were accurately quantified by simulating the BRN until all states reached stability.

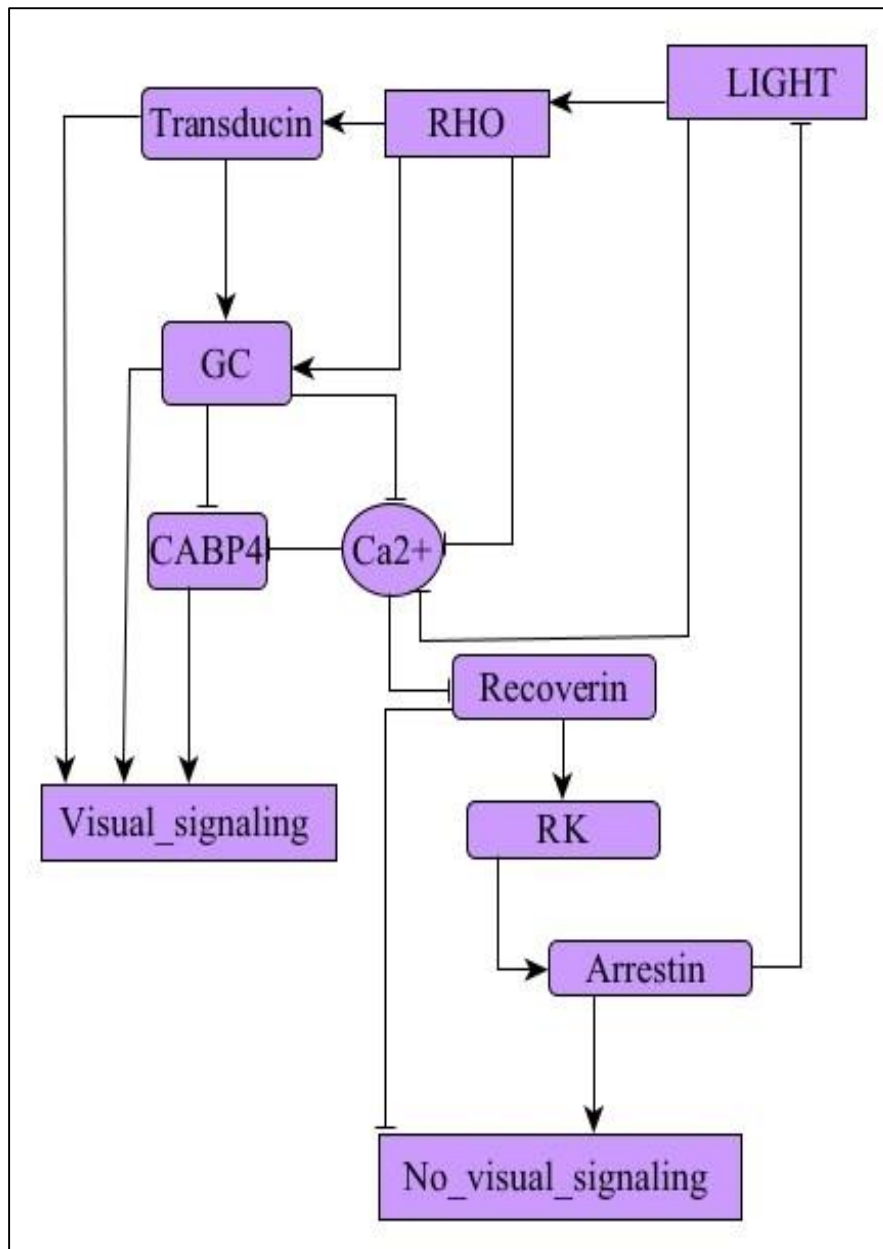


**Figure 10: Biological Regulatory Network for visual signaling in response to light (61).**

Dynamic simulations were conducted on a normal cascade to maintain a low activation range (0.0) for each node. To assess the  $\text{Ca}^{2+}$  and CABP4 responses, the light concentration was incrementally increased to a moderately active state (0.5). Subsequently, the light concentration was further increased to a hyperactive state (1.0) to observe the  $\text{Ca}^{2+}$  and CABP4 responses, as well as the activation of GC and RHO as shown in simulation part in Figure 11.

## 4.2 Normal Visual Signaling Simulations in Light Response:

During the simulation, light-activated a signaling cascade involving the proteins. The changes in light concentration triggered significant changes in their expression levels, suggesting their essential roles as primary regulators in the visual signaling cascade. The light activated the RHO which send positive signals to Transducin at a moderate level throughout the simulation which was 50 seconds. The Transducin is the further activator of GC throughout each time step, both Transducin and GC gradually increased in expression until reaching a moderately active level (0.775 and 0.972, respectively). At this stage,  $\text{Ca}^{2+}$  values ranged from 0.036 to 0.012, while CABP4 values varied from 0.01 to 0.03, as shown in the Figure 11(a). The fluctuations observed in  $\text{Ca}^{2+}$  and CABP4 levels reflected their crucial functions as mediators, modulating the signal transmission to the brain in a time-sensitive manner.

Moreover, Transducin was found to increase the expression of GC, leading to an oscillating curve and a peak GC expression of 0.97, as shown in Figure 11(a). At this point, both  $\text{Ca}^{2+}$  and CABP4 concentrations were inhibited, producing a positive response in visual signaling. The inhibition of  $\text{Ca}^{2+}$  at the inactive level (0.036) gave rise to negative signals that affected Recoverin. The complicated interaction between Recoverin and Rhodopsin kinase (RK) showed a positive feedback loop in the light response. The inhibition of Recoverin, in turn, further activated Rhodopsin kinase (RK) at a moderately active level (0.94), sending positive signals to Arrestin activation (0.97) throughout the simulation (ranging from 0.00 to 0.943). The activation of Arrestin at a moderately active level played a key role in controlling the expression of RHO, which is a photoactivated receptor in the visual mechanism. This controlled mechanism of the photoreceptor was necessary for the recovery of light response to ensure the system's ability to return to its baseline state after exposure to light as shown in the Figure 11(c).

**Table 2: Parameters values of entities interacting with Ca<sup>2+</sup> and CABP4 in light before and after simulation generated by Jimena.**

Normal visual signaling in light						
Nodes	Light value 0 ( Normal Activation of visual signaling)		light value 0.5 (Normal Activation of visual signaling )		light value 1 (Normal Activation of visual signaling )	
	Before simulation	After simulation	Before simulation	After simulation	Before simulation	After simulation
Arrestin	0	0.943	0	0.956	0	0.949
CABP4	0	0.073	0	0.072	0	0.072
Ca <sup>2+</sup>	0	0.036	0	0.042	0	0.039
GC	0	0.972	0	0.959	0	0.968
Light	0	0.084	0.5	0.064	1	0.074
No-Visual Signaling	0	0.007	0	0.005	0	0.006
RHO	0	0.283	0	0.221	0	0.252
RK	0	0.962	0	0.97	0	0.966
Recoverin		0.97		0.975	0	0.972
Transducin	0	0.775	0	0.656	0	0.721
Visual signaling	0	0.972	0	0.973	0	0.973

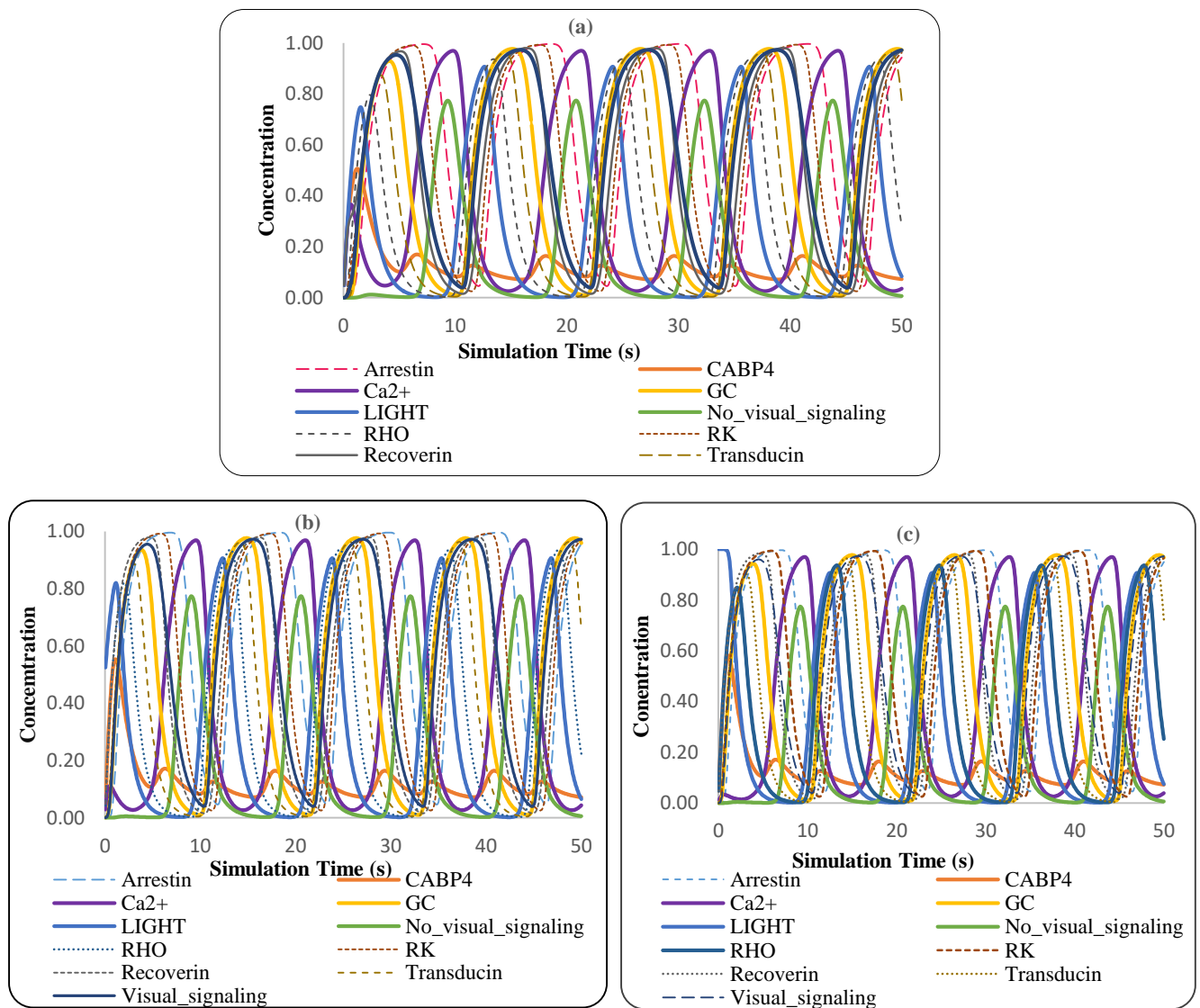


**Figure 11: Jimena's dynamic simulation of the visual signaling pathway in light and the inhibitory effect on CABP4 and Ca<sup>2+</sup> concentrations, controlling the mechanism of light response. The x-axis represents the simulation time in seconds, while the y-axis indicates the relative concentration of activators and inhibitors. The three scenarios are presented as follows: (a) Simulation results with light in its inactive initial state. (b) Simulation outcomes when light is initially in the active state. (c) Simulated results when light is maintained in its hyperactive state.**

### 4.3 Biological Regulatory Network (BRN) Construction of Visual Signaling for Dark Response:

The BRN was designed to explore the mechanism of  $\text{Ca}^{2+}$  and its interactions with other proteins in low-light conditions/dark. The simulation focused on visual response as the main outcome. The downstream signaling target in this BRN was GCAP. A reduction in  $\text{Ca}^{2+}$  concentrations occurs as a result of ion channels remaining closed in light conditions, which leads to a decrease in GCAP activity (62). Inhibition of GCAP restores cGMP concentration and opens cyclic nucleotide ion channels in dark/low light conditions. Consequently, the opening of ion channels leads to an elevation in  $\text{Ca}^{2+}$  concentration, resulting in membrane depolarization. This depolarization transmits signals to the brain for processing in response to low light conditions. The higher calcium levels subsequently trigger the activation of calcium-binding proteins, including CABP4 and recoverin (35).

In conditions of low light, both  $\text{Ca}^{2+}$  and CABP4 serve as positive mediators of signaling. The activation of CABP4 facilitates the passage of calcium through L-type Cav1.4 channels, aiding in the release of neurotransmitters from the presynaptic membrane. These neurotransmitters then bind to postsynaptic glutamate receptors, transmitting signals to nerve cells (35). The other protein, Recoverin interacts with Rhodopsin kinase and regulates the rate of rhodopsin phosphorylation, affecting the lifespan of Rho. When  $\text{Ca}^{2+}$  concentration decreases, arrestin dissociates from GRK, leading to increased kinase activity, as shown in the Figure 12 (63).

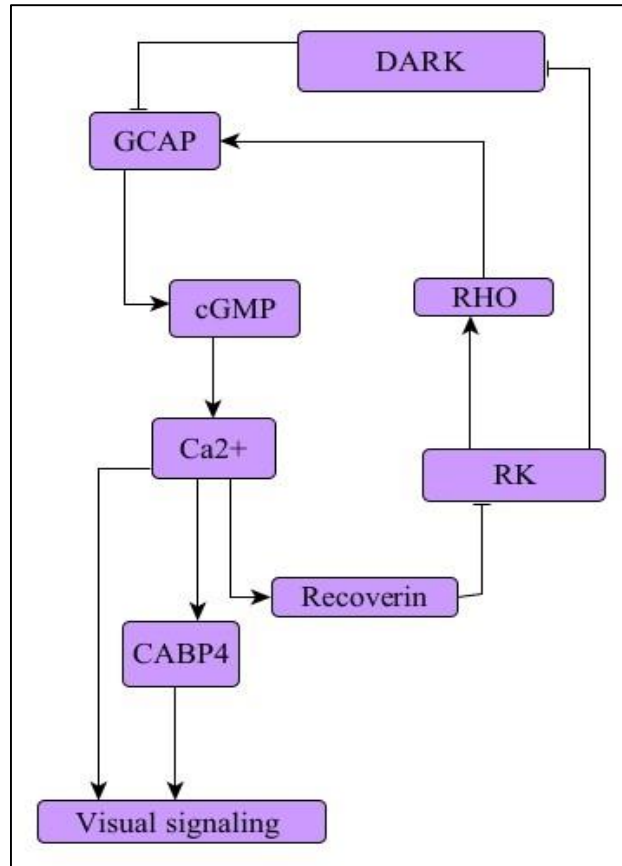


**Figure 12: Biological Regulatory Network for visual signaling in response to dark (50).**

#### 4.4 Normal Visual Signaling Simulations in Dark Response:

During the simulation, we observed that cGMP activation remained at a moderately active level due to the inhibition of GCAP, as shown in Figure 10(a). In the absence of light, GCAP was consistently inhibited at 0.06 as shown in Table 3. The activation of cGMP in the range of 0.4 to 0.8 effectively opened the CNG ion channels, allowing ions to enter and facilitating the transmission of signals within the visual system.

Moreover, the positive effects of cGMP resulted in the activation of CABP4 and a gradual increase in  $\text{Ca}^{2+}$  levels. Both  $\text{Ca}^{2+}$  and CABP4 expression levels steadily rose until they reached moderate activation levels, with values of 0.95 and 0.85, respectively. This suggests that the increasing concentrations of  $\text{Ca}^{2+}$  and CABP4 during the simulation played a significant role in regulating and controlling the visual signaling pathway.

Additionally, the BRN was tested at various  $\text{Ca}^{2+}$  levels as shown in Figure 10(b). At an initial value of 0.5, which acts as the activator of visual response in dark conditions, both CABP4



and visual signaling exhibited oscillatory behavior. Starting from low levels of 0.01, they gradually increased to 0.04, eventually reaching a more active state at 0.82. This observation suggests that the BRN and the visual signaling pathway were sensitive to changes in  $\text{Ca}^{2+}$  levels, displaying dynamic behavior in response to the initial activation of visual response in dark conditions.

Furthermore, in a separate simulation where the BRN was tested at a hyperactive state of  $\text{Ca}^{2+}$ , as shown in Figure 10(c), both CABP4 and visual signaling reached their maximum activation state at an early point. This indicates that the visual signaling pathway and the activation of CABP4 were dependent on changes in  $\text{Ca}^{2+}$  levels, quickly achieving their maximum potential for activation.

**Table 3: Parameters values of entities interacting with  $\text{Ca}^{2+}$  in dark before and after simulation generated by Jimena.**

Normal visual signaling in Dark						
Nodes	Dark ( Normal Activation of visual signaling)		$\text{Ca}^{2+}$ value 0.5 (Normal Activation of visual signaling )		$\text{Ca}^{2+}$ value 1 (Normal Activation of visual signaling )	
	Before simulation	After simulation	Before simulation	After simulation	Before simulation	After simulation
CABP4	0	0.265	0	0.288	0	0.972
$\text{Ca}^{2+}$	0	0.08	0.5	0.087	1	0.572
Dark	0	0.95	0	0.966	0	0.95
GCAP	0	0.006	0	0.006	0	0.052
RHO	0	0.05	0	0.034	0	0.05
RK	0	0.249	0	0.209	0	0.014
Recoverin	0	0.265	0	0.288	0	0.972
Visual Signaling	0	0.672	0	0.712	0	0.988
cGMP	0	0.023	0	0.025	0	0.185

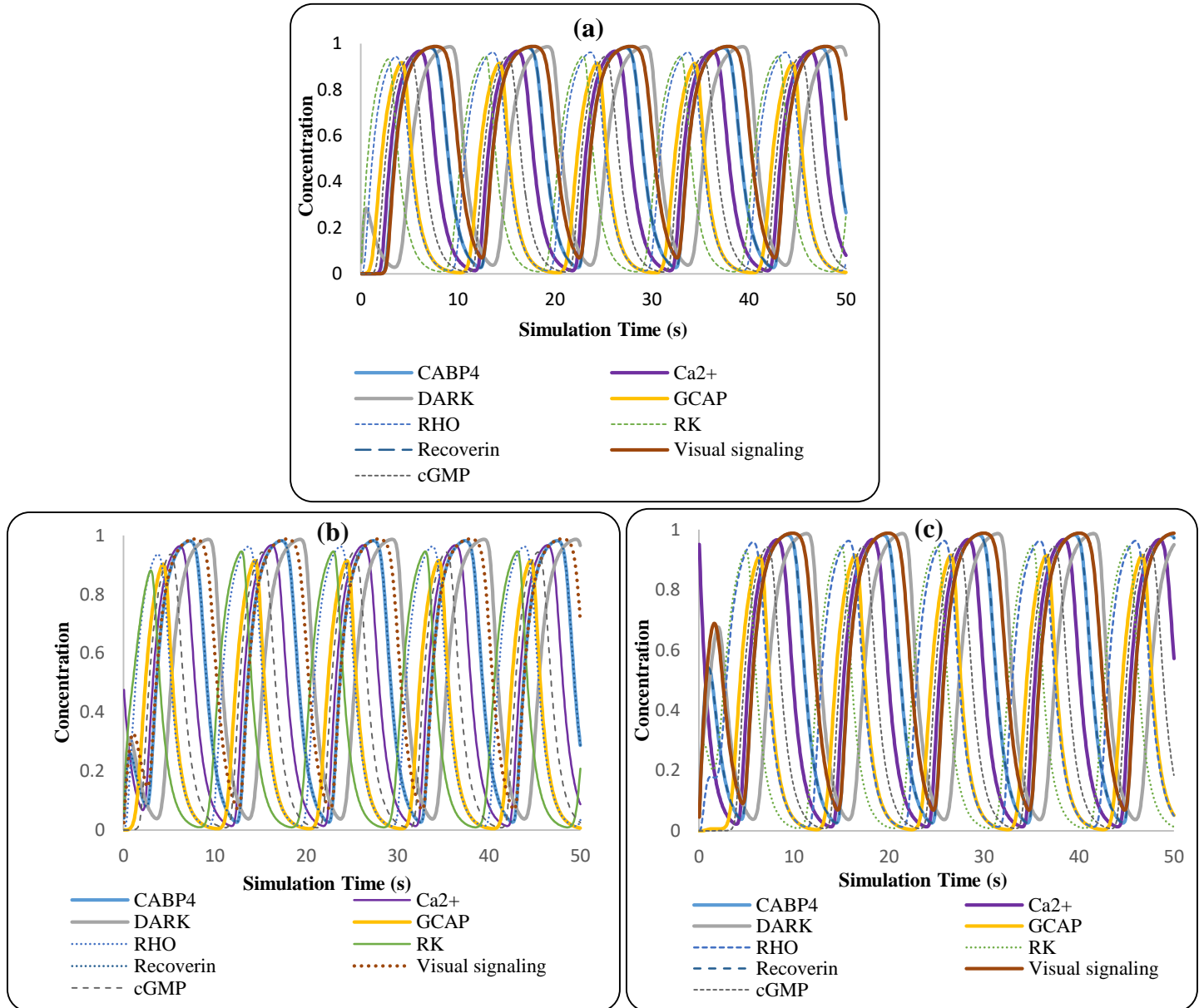


**Figure 13:** The results of Jimena's dynamic simulation of the visual signaling pathway in dark conditions, focusing on the role of activators in regulating CABP4 and Ca<sup>2+</sup> concentrations to control the mechanism of dark response. The x-axis represents simulation time in seconds, while the y-axis indicates the relative concentration of activators and inhibitors. The study explores three scenarios: (a) Simulation results when the cascade is in the initial state in the dark mechanism. (b) Simulation outcomes when Ca<sup>2+</sup> is initially in the active state. (c) Simulated results when Ca<sup>2+</sup> is maintained in its hyperactive state.

The Dark BRN was tested at different concentrations of CABP4 (0.5 and 1.0) during a 50-second simulation. The initial value of CABP4 was set to 0.5, while all other nodes were kept at an inactive value of 0.0. The simulation results revealed a significant difference in the activation values before and after the simulation. With a CABP4 value of 0.5, there was a noticeable change in visual signaling compared to normal visual signaling, particularly in low-light conditions, as shown in Figure 14(a). The visual response showed hyperactive behavior during the BRN simulation when CABP4 was set to 1.0. As a consequence, the visual signal reached a hyperactive value of 0.9. These findings suggest that CABP4 plays an essential role in transmitting signals to the brain for visual responses, as shown in Table 4.

**Table 4: Parameters values of entities interacting with CABP4 in dark before and after simulation generated by Jimena.**

<b>Normal visual signaling in Dark</b>				
<b>Nodes</b>	<b>CABP4 value 0.5 (Normal Activation of visual signaling )</b>		<b>CABP4 value 1 (Normal Activation of visual signaling )</b>	
	<b>Before simulation</b>	<b>After simulation</b>	<b>Before simulation</b>	<b>After simulation</b>
<b>CABP4</b>	0.5	0.265	1	0.265
<b>Ca<sup>2+</sup></b>	0	0.08	0	0.08
<b>Dark</b>	0	0.95	0	0.95
<b>GCAP</b>	0	0.006	0	0.006
<b>RHO</b>	0	0.05	0	0.05
<b>RK</b>	0	0.249	0	0.249
<b>Recoverin</b>	0	0.265	0	0.265
<b>Visual Signaling</b>	0	0.675	0	0.672
<b>cGMP</b>	0	0.023	0	0.023

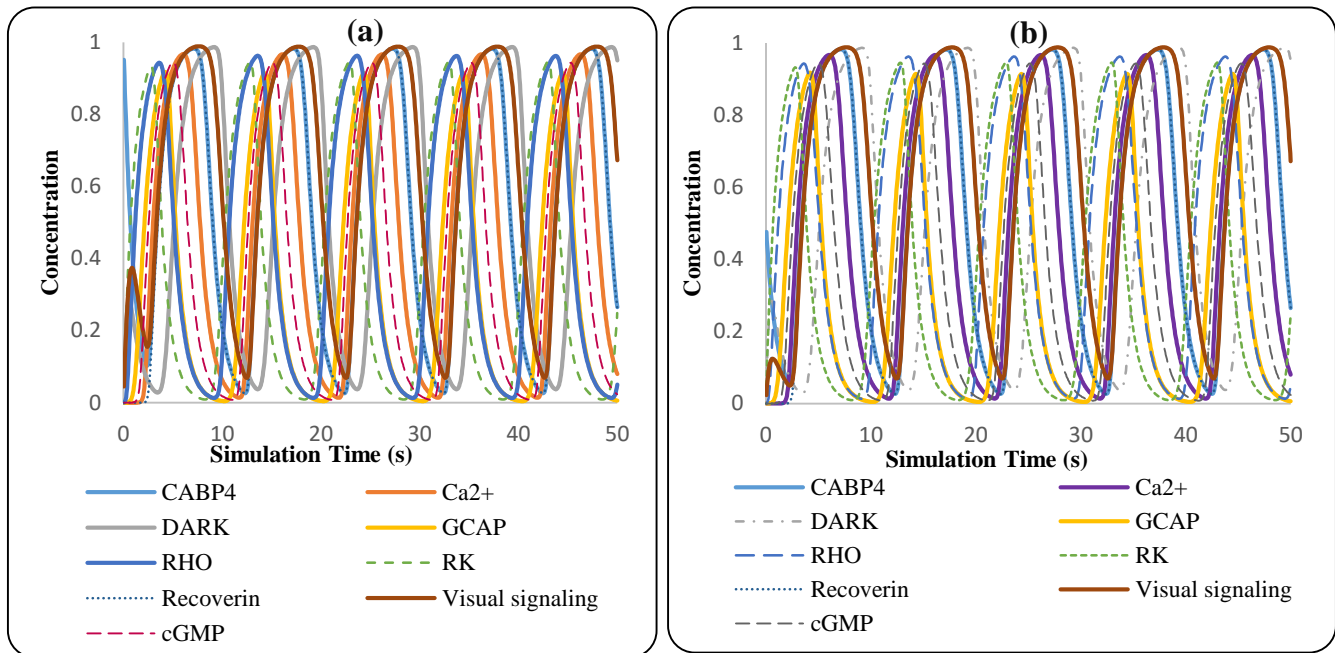


**Figure 14:** The results of Jimena's dynamic simulation of the visual signaling pathway in dark conditions reveal the effect of CABP4 on the regulation of visual response in dark conditions. The x-axis represents simulation time in seconds, while the y-axis indicates the relative concentration of activators and inhibitors. The study explores two scenarios (a) Simulation outcomes when CABP4 is initially in the active state. (b) Simulated results when CABP4 is maintained in its hyperactive state

#### 4.5 Biological Regulatory Network (BRN) Construction for Night Blindness:

In certain disease conditions like congenital stationary night blindness is due to the impaired function of the calcium-binding protein CABP4 (calcium-binding protein 4)(24). Consequently, the elevated concentration of  $\text{Ca}^{2+}$  ions leads to further depolarization of the membrane potential as discussed in the literature review section(25).

This depolarization significantly disrupts the processing of photoreceptor signals and directly affects the transmission of signals from rod photoreceptors to retinal bipolar cells(64). The BRN was constructed to analyze the behavior of CABP4 and  $\text{Ca}^{2+}$  on visual signaling in disease conditions.

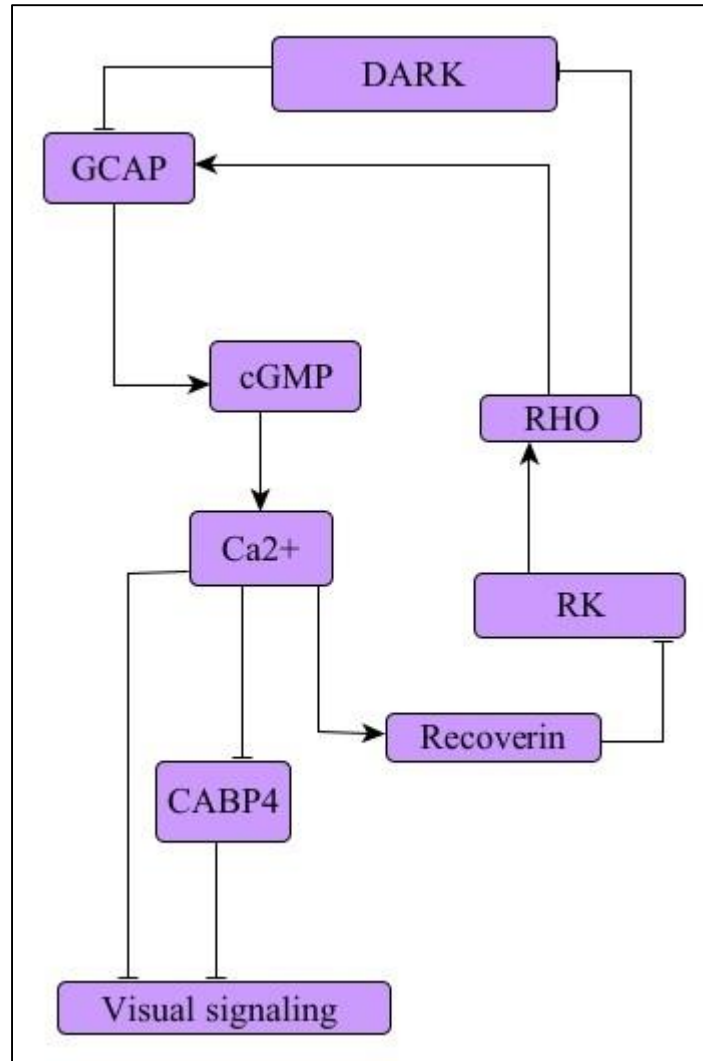


**Figure 15: Biological Regulatory Network for visual signaling in Night-Blindness(24, 25).**

#### 4.6 Visual Signaling Simulations in Night-Blindness:

The visual cascade associated with night blindness includes BRN where CABP4 functions as a negative regulator in visual signaling. In disease condition, the role of  $\text{Ca}^{2+}$  and CABP4 was investigated by initializing all nodes with an inactive value of 0.0 in BRN. The simulation was conducted for 50 seconds to observe the activation levels of visual signaling in the diseased state compared to normal visual signaling. During the simulation, it was found that in the disease condition, the value of  $\text{Ca}^{2+}$  was hyperactive, reaching a concentration of 0.85. However, the visual response remained in a low activation state, ranging from 0.2 to 0.35, throughout the entire simulation, as shown in Table 5. The most significant difference observed in this simulation was

related to CABP4. Unlike the normal state, CABP4 did not show hyperactivity in the disease condition. Instead, its concentration dropped to 0.16 during the simulation, as shown in the Figure 16.

The BRN was tested with  $\text{Ca}^{2+}$  values of 0.5 and 1.0, while all other nodes remained inactive (0.0). Interestingly, even at a moderate activation level (0.5) of  $\text{Ca}^{2+}$ , there was insufficient upregulation of CABP4 concentration, resulting in the visual response remaining at a lower active state (0.35), as shown in Figure 17. Similarly, when  $\text{Ca}^{2+}$  was set to a hyperactive state of 1.0 during the simulation, the visual response showed the same outcome, remaining at a lower activation state (0.35). This suggests that in the disease state, the dysregulation of CABP4 might be a critical factor contributing to the reduced visual response despite the hyperactive  $\text{Ca}^{2+}$  concentration.

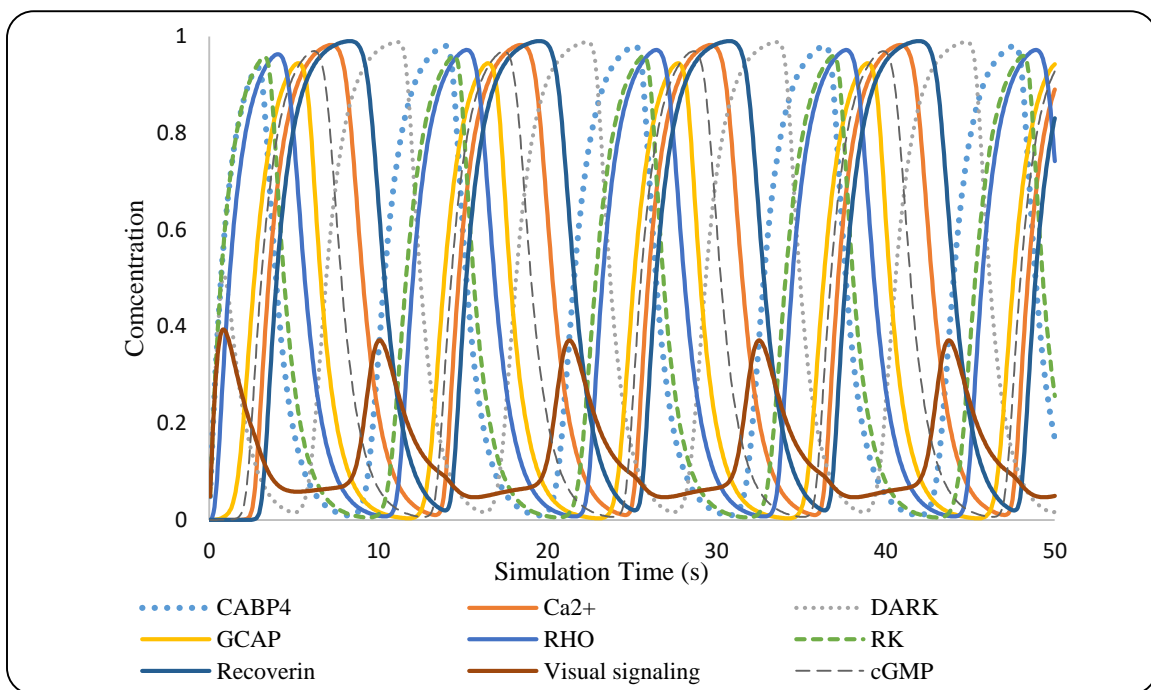


**Figure 16: Dynamic simulation of night-blindness.**

**Table 5: Parameters values of entities interacting with  $\text{Ca}^{2+}$  in night-blindness before and after simulation generated by Jimena.**

<b>Night Blindness Visual Signaling</b>						
<b>Nodes</b>	<b>Dark (Night Blindness)</b>		<b><math>\text{Ca}^{2+}</math> value 0.5 (Night Blindness )</b>		<b><math>\text{Ca}^{2+}</math> value 1 (Night Blindness )</b>	
	<b>Before simulation</b>	<b>After simulation</b>	<b>Before simulation</b>	<b>After simulation</b>	<b>Before simulation</b>	<b>After simulation</b>
CABP4	0	0.169	0	0.184	0	0.913
$\text{Ca}^{2+}$	0	0.89	0.5	0.88	1	0.327
DARK	0	0.016	0	0.016	0	0.078
GCAP	0	0.942	0	0.94	0	0.685
RHO	0	0.742	0	0.782	0	0.949
RK	0	0.257	0	0.279	0	0.96
Recoverin	0	0.831	0	0.816	0	0.087
Visual Signaling	0	0.049	0	0.049	0	0.07
cGMP	0	0.928	0	0.922	0	0.548

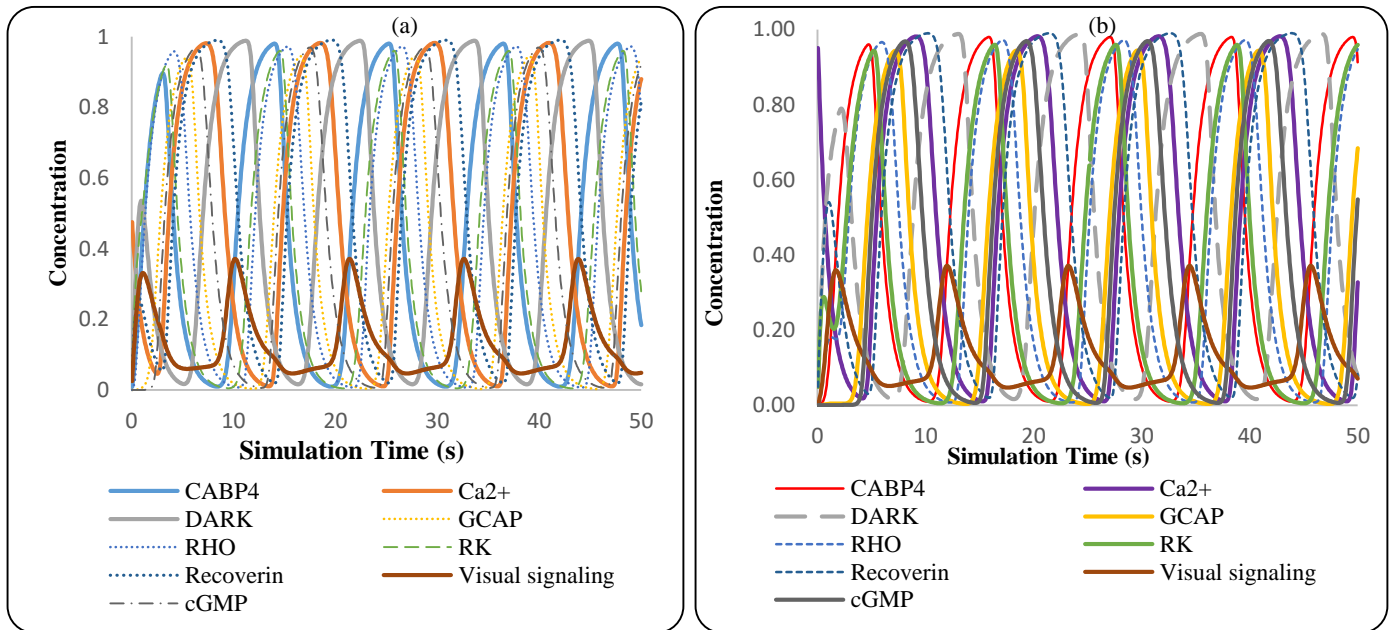


**Figure 17: Dynamic simulation of BRN moderate active and hyperactive  $\text{Ca}^{2+}$  in night-blindness.**

The role of CABP4 in night blindness was studied at different concentrations, including 0.5 (moderate activation) and 1.0 (hyperactive), while all other nodes were kept in an inactive state (0.0). The simulation was run for 50 seconds. During the simulation, it was observed that the  $\text{Ca}^{2+}$  concentration became hyperactive at 0.3 seconds.

However, the CABP4 concentration only reached a hyperactive state at 0.1 seconds, as shown in Figure 15(a). As a result, the visual signaling response remained at a lower active state (0.1) at this time step. This pattern was consistently repeated in both hyperactive and moderate active CABP4 conditions, indicating that the visual signaling response remained lower active in night blindness regardless of the CABP4 concentration. These findings suggest that in night blindness, the dysregulation of CABP4 may play a crucial role in impairing the visual response, leading to the observed lower activation state in the visual signaling pathway.



**Table 6: Parameters values of entities interacting with CABP4 in night blindness before and after simulation generated by Jimena.**

Normal visual signaling in Dark				
Nodes	CABP4 value 0.5 (Night Blindness)		CABP4 value 1 (Night Blindness)	
	Before simulation	After simulation	Before simulation	After simulation
CABP4	0.5	0.169	1	0.169
Ca <sup>2+</sup>	0	0.89	0	0.89
Dark	0	0.016	0	0.016
GCAP	0	0.942	0	0.942
RHO	0	0.742	0	0.742
RK	0	0.257	0	0.257
Recoverin	0	0.831	0	0.831
Visual Signaling	0	0.049	0	0.049
cGMP	0	0.928	0	0.928

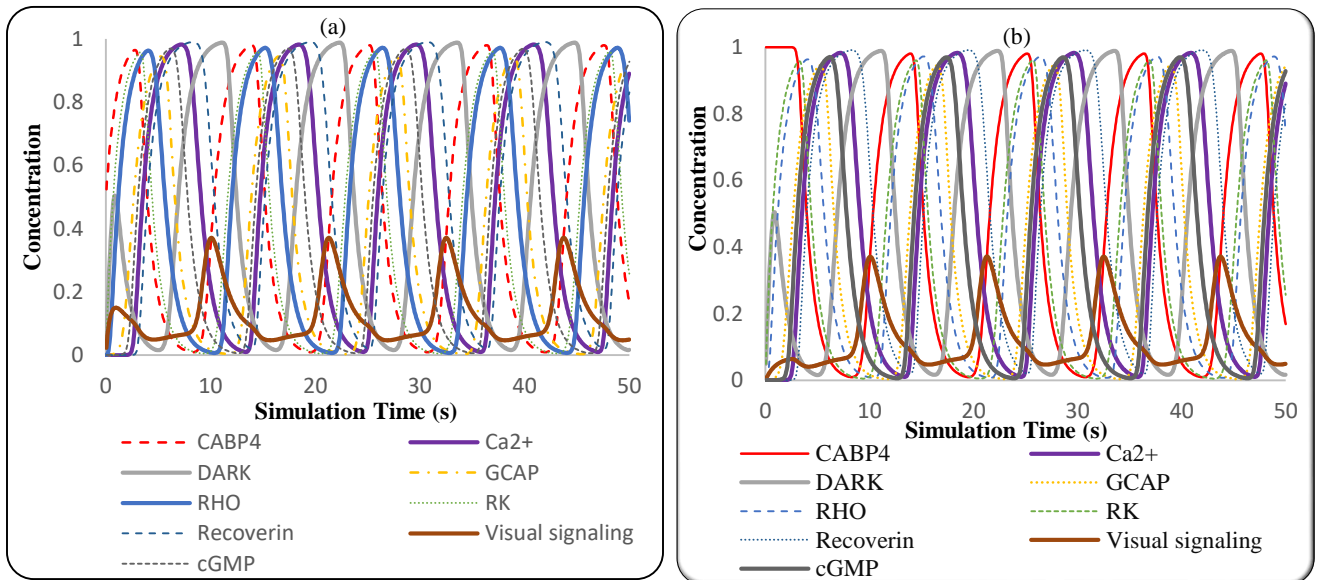


**Figure 18: Dynamic simulation of BRN moderate active and hyperactive CABP4 in night-blindness.**

The BRN was first perturbed with hyperactive CABP4 (1.0) and moderately active  $\text{Ca}^{2+}$  (0.5), and simulated for 50 seconds. As discussed earlier,  $\text{Ca}^{2+}$  activates CABP4, which regulates signal transmission. However, in this perturbed condition, both  $\text{Ca}^{2+}$  and CABP4 showed dysregulation, leading to a disease-like state where visual signals were not properly transmitted to the brain throughout the entire simulation. In the second condition, the BRN was tested with perturbation only on  $\text{Ca}^{2+}$  to assess its sensitivity. The hyperactive calcium failed to activate CABP4, and as a result, CABP4 remained in a low active state. The perturbation with hyperactive  $\text{Ca}^{2+}$  caused the visual signaling peak to remain at 0.077, indicating a low active state. These simulation results strongly support the hypothesis that  $\text{Ca}^{2+}$  is a sensitive parameter in night blindness disease. Changes in  $\text{Ca}^{2+}$  concentration directly impact the activation of CABP4 and the transmission of visual signaling in the disease condition. Understanding the complex interplay between  $\text{Ca}^{2+}$  and CABP4 in visual signaling may pave the way for potential therapeutic interventions to address night blindness and related visual disorders.

**Table 7: Parameters values of entities perturbation CABP4 and  $\text{Ca}^{2+}$  before and after simulation generated by Jimena**

Nodes	CABP4 Perturbation		$\text{Ca}^{2+}$ Perturbation	
	Before simulation	After simulation	Before simulation	After simulation
CABP4	1	1	0	0.001
$\text{Ca}^{2+}$	0.5	0.5	1	1
Dark	0	1	0	1
GCAP	0	0	0	0
RHO	0	0.002	0	0
RK	0	0.01	0	0
Recoverin	0	0.83	0	0.999
Visual Signaling	0	0.013	0	0.077
cGMP	0	0	0	0

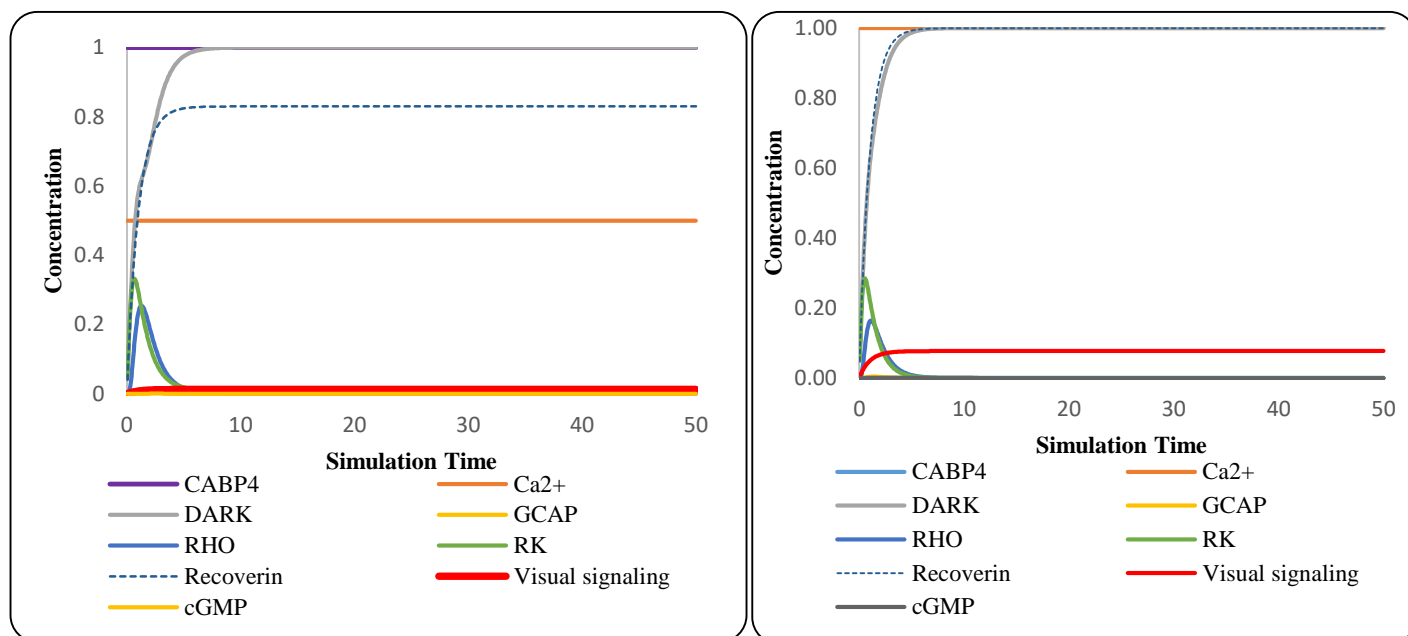


**Figure 19: Dynamic simulation of BRN in perturbed with CABP4 and  $\text{Ca}^{2+}$  concentration leading towards the no visual singling.**

#### 4.7 Analysis of Stable Structures after Simulation

In the preceding sections, simulations were conducted to assess the stability of both the Wild-type and Mutant-CABP4 proteins. The Wild-type CABP4 achieves stability after about 35 nanoseconds and maintains its stability throughout the entire 100-nanosecond simulation, with an RMSD ranging from 2 to 2.45 Å, as shown in Figure section 20. After a 100ns simulation of the Mutant-CABP4, a small RMSD between 0.5-1.25 Å was observed, indicating a stable conformation that enables the protein to perform its functionality, as depicted in the Figure 20. Similarly, the IQ-motif, obtained from homology modeling, underwent a 100ns simulation to assess its stability. During this simulation, the best stable conformation was achieved within the range of 0.5-1.5 RMSD value, as depicted in the Figure 20, ensuring its suitability for further analysis and study.

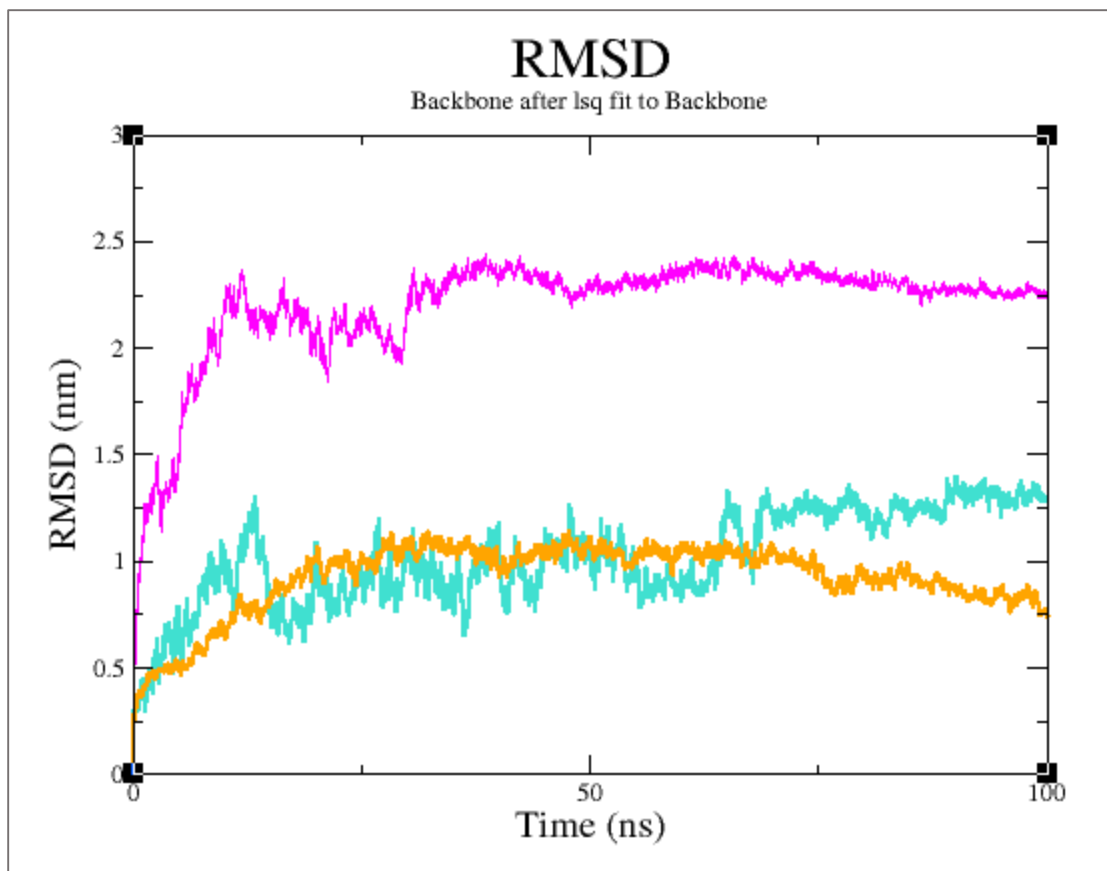


**Figure 20: The RMSD graph after simulation of Wild-type CABP4, Mutant-CABP4 and IQ-motif. The stability of Wild-type CABP4 is depicted by the magenta trajectory color, while the cyan color in the figure represents the RMSD of the IQ motif. Additionally, the orange color illustrates the RMSD stability of the mutant CABP4, as shown in the figure.**

## 4.8 Molecular Docking

We investigated the interaction between wild-type CABP4 and its receptor IQ motif, as well as mutant CABP4 and its receptor IQ motif, using the HADDOCK algorithm. The best stable 3D structures were obtained through simulation with GROMACS, which were then used as input for the HADDOCK server. From the docking results, we selected the top-ranked cluster based on RMSD from the overall lowest energy structure, and z-scores. Both the wild-type and mutant complexes docked with the IQ motif were analyzed. The following tables presents the number of generated top 5 clusters along with their corresponding RMSD, lowest energy values, and z scores. A smaller RMSD value suggests a higher structural similarity to the overall lowest energy structure. Negative values in energy scores signify favorable interactions that contribute to the

stability of the complex. Additionally, a more negative Z-score indicates a higher quality of docking, reflecting a better fit of the docking prediction to experimental data.

**Table 8: Top 5 Clusters with RMSD, lowest energy score, and z- Score for Mutant docked complex.**

Cluster	RMSD	Lowest energy Kcal/mol	z-score
1	3.9	-77.5	-0.6
2	12.4	-79.2	-0.2
3	12.4	-71.2	0.2
4	10.1	-83.2	0.4
5	7.8	-67.6	1.1

**Table 9: Top 5 Clusters with RMSD, lowest energy score, and z- Score for Wild-type docked complex.**

Cluster	RMSD	Lowest energy Kcal/mol	z-score
1	9.9	-67.7	-1.5
2	12.7	-70.5	-0.9
3	9.9	-68.7	-0.9
4	8.4	-76.81	-0.7
5	1.6	-56.6	-0.5

#### 4.9 Interaction between the Molecules of Wild-type Docked Complex

As discussed in the literature review section, the initial 99 residues of CABP4 were identified as a loop region, which was not involved in the protein functionality. Consequently, these loop regions were removed after conducting simulations, and the remaining structure was then docked with IQ motif by HADDOCK. The docked complex of Wild-type CABP4-IQ consists of 75 residues of the IQ motif and 176 residues of Wild-type CABP4 (residues 100-275), showing their interaction with each other.

This complex is characterized by 14 hydrogen bond interactions, as shown in Figure 19. Particularly, specific residues of Wild-type CABP4, including Gly162, Val208, His204, Met205, Arg212, Leu257, Asn258, Thr262, Asp264, Asp266, Ser273, and His275, were found to participate in hydrogen bond interactions with the IQ-motif, as shown in the Figure 19. These interactions are crucial for the functionality of Cav1.4. They play a vital role in maintaining the calcium channel open in dark conditions, particularly at higher  $\text{Ca}^{2+}$  levels, and facilitate the transmission of signals to the brain for visual processing in low-light situations.

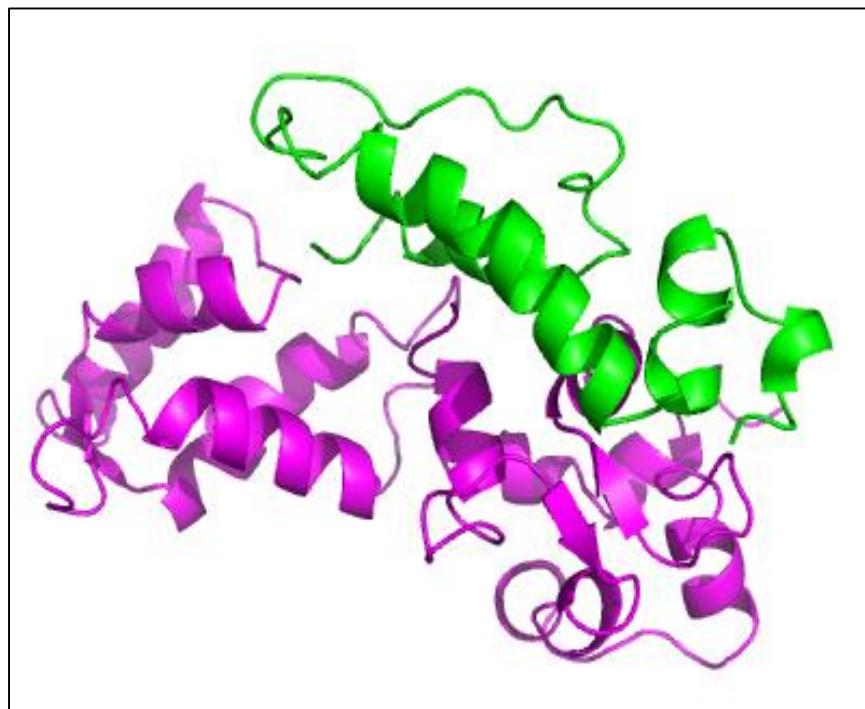


**Figure 21: Visualization of Wild-type CABP4-IQ Docked Complex using Pymol Software. In the visualization, the IQ-motif is highlighted in green, while the Wild-type CABP4 is depicted in magenta color.**

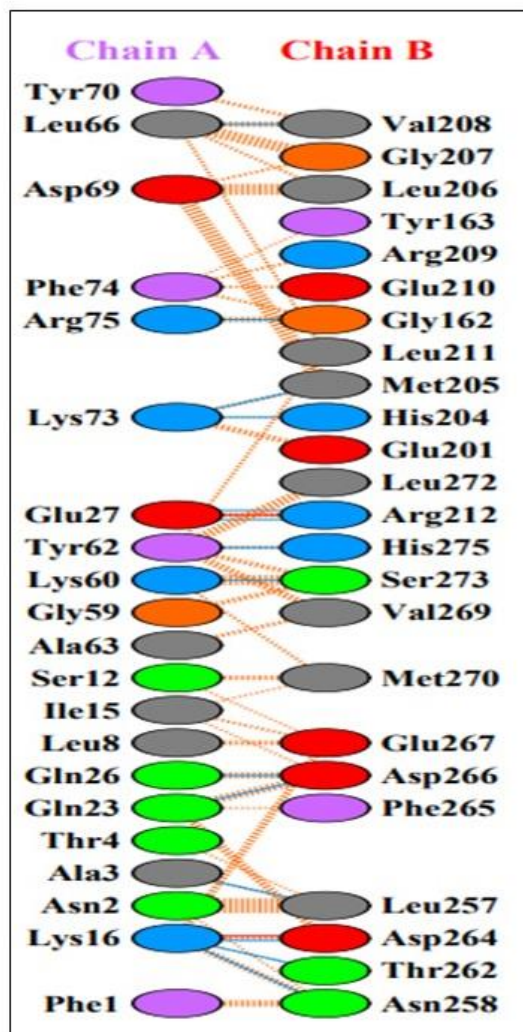


**Figure 22:** The interacting residues between the IQ-motif (Chain A) and Wild-type CABP4 (Chain B) within the docked complex are identified using data from pdbsum.

#### 4.10 Interaction between the Molecules of Mutant Docked Complex

The Mutant CABP4-IQ docked complex comprises 75 residues of IQ and 258 residues of Mutant-CABP4(100-357), showing distinct interactions between them. The complex involves a total of 12 hydrogen bond interactions. Notably, the Mutant-CABP4 residues Arg100, Gln109, Arg110, Asn117, Thr166, Glu169, Glu172, Leu193, His204, Glu241, and Lys342 participate in these hydrogen bond interactions with IQ-motif, as shown in the Figure 23.

However, in this Mutant Docked complex, there were no interactions observed involving the essential residues of the fourth EF-Domain. These residues are crucial for binding with the IQ motif of Cav1.4. As a result of this mutation, the binding with calcium channels becomes disrupted

and inadequately regulated under the mutant CABP4. Consequently, this condition leads to night blindness.

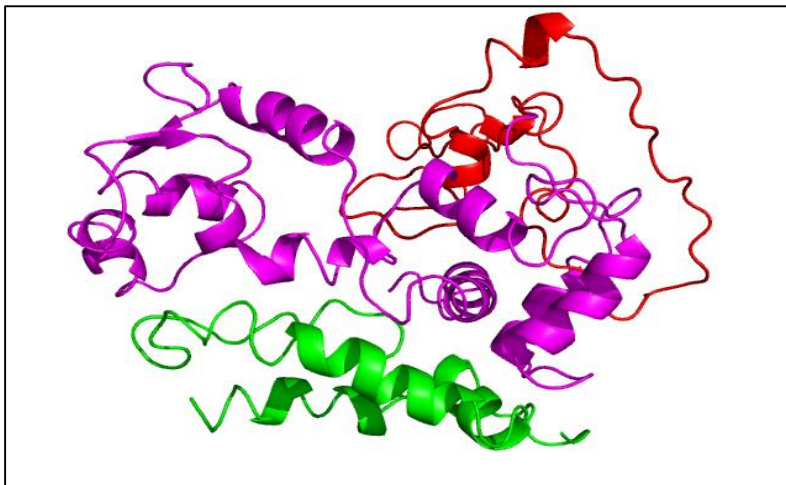


**Figure 23:** Visualization of Mutant CABP4-IQ docked complex using pymol Software. In the visualization, the IQ-motif is highlighted in green, while the Mutant-CABP4 is depicted in magenta color.

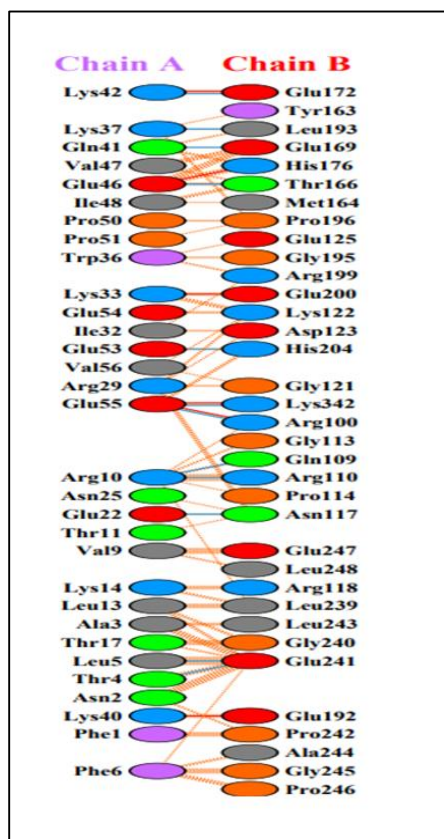


**Figure 24:** The interacting residues between the IQ-motif (Chain A) and Mutant-CABP4 (Chain B) within the docked complex are identified using data from pdbsum.



### 4.11 MD Simulation Analysis

Following the docking process, we performed simulations to assess the stability of the Wild-type CABP4-IQ complex and Mutant CABP4-IQ complex throughout 100ns. To estimate the complexes stability, we calculated the Root Mean Square Deviation (RMSD) of the protein backbone. The analysis revealed that the structure of the Wild-type CABP4-IQ complex remained consistently stable within an RMSD range of 0.4 to 0.5Å, while the Mutant CABP4-IQ complex trajectory showed fluctuation within an RMSD range of 0.2 to 0.8Å, as shown in Figure 25.

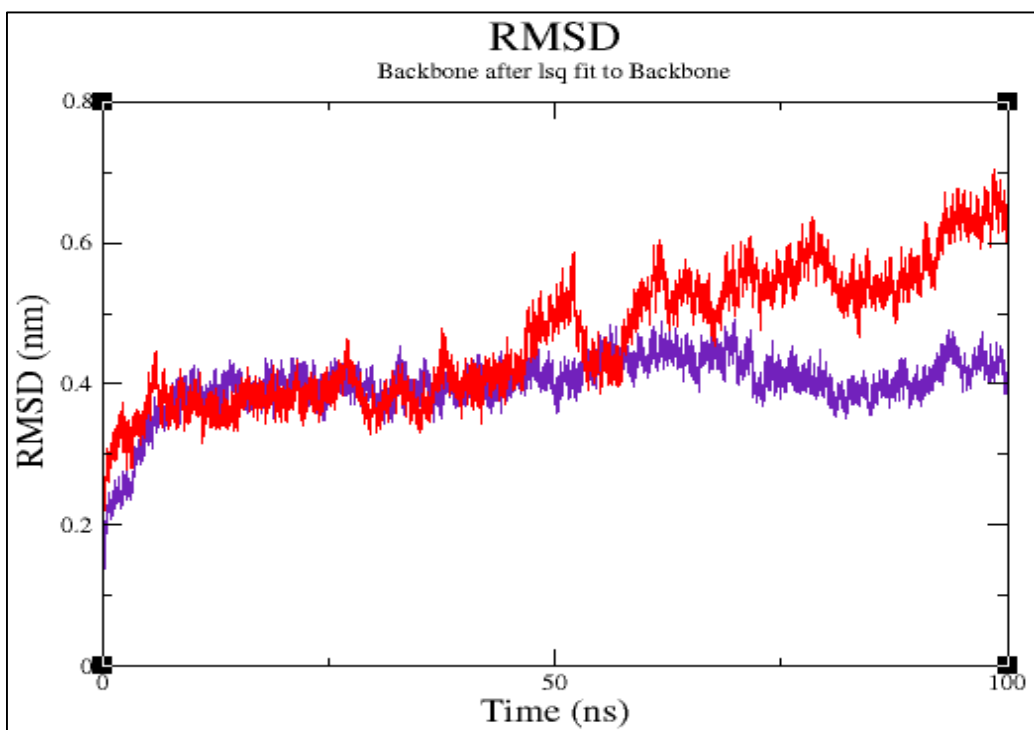


**Figure 25: Comprehensive analysis of the molecular dynamics (MD) simulation performed on the Wild-type CABP4-IQ and Mutant CABP4-IQ complexes. In the figure, the RMSD of the Mutant CABP4 IQ complex is indicated by the red color, while the purple color denotes the RMSD of the Wild-type CABP4-IQ complex.**

Consequently, we proceeded to analyze the fluctuation of residues within the protein trajectories for both wild-type CABP4-IQ complex and Mutant CABP4-IQ complex by determining the Root Mean Square Fluctuation (RMSF), as shown in the same Figure 26. The RMSF graphs indicate the residues showing significant fluctuations in the structure. The residues

that are highly fluctuated in the structure are labeled in the RMSF graphs. Before the docking process, the initial 100 amino acid residues were excluded from the protein structure. These residues were situated within the N-terminus loop region of the protein and were determined to be unrelated to the protein's functionality based on literature findings. This exclusion was supported by the fact that it did not impact the calcium binding interaction with the EF domain of CABP4. The graph displayed below illustrates the residual fluctuations of amino acid residues. Specifically, it portrays residues 1 to 75 of the IQ motif, residues 100 to 275 of the Wild-type CABP4, and residues 100 to 357 of the Mutant CABP4 within the docked complex (29).

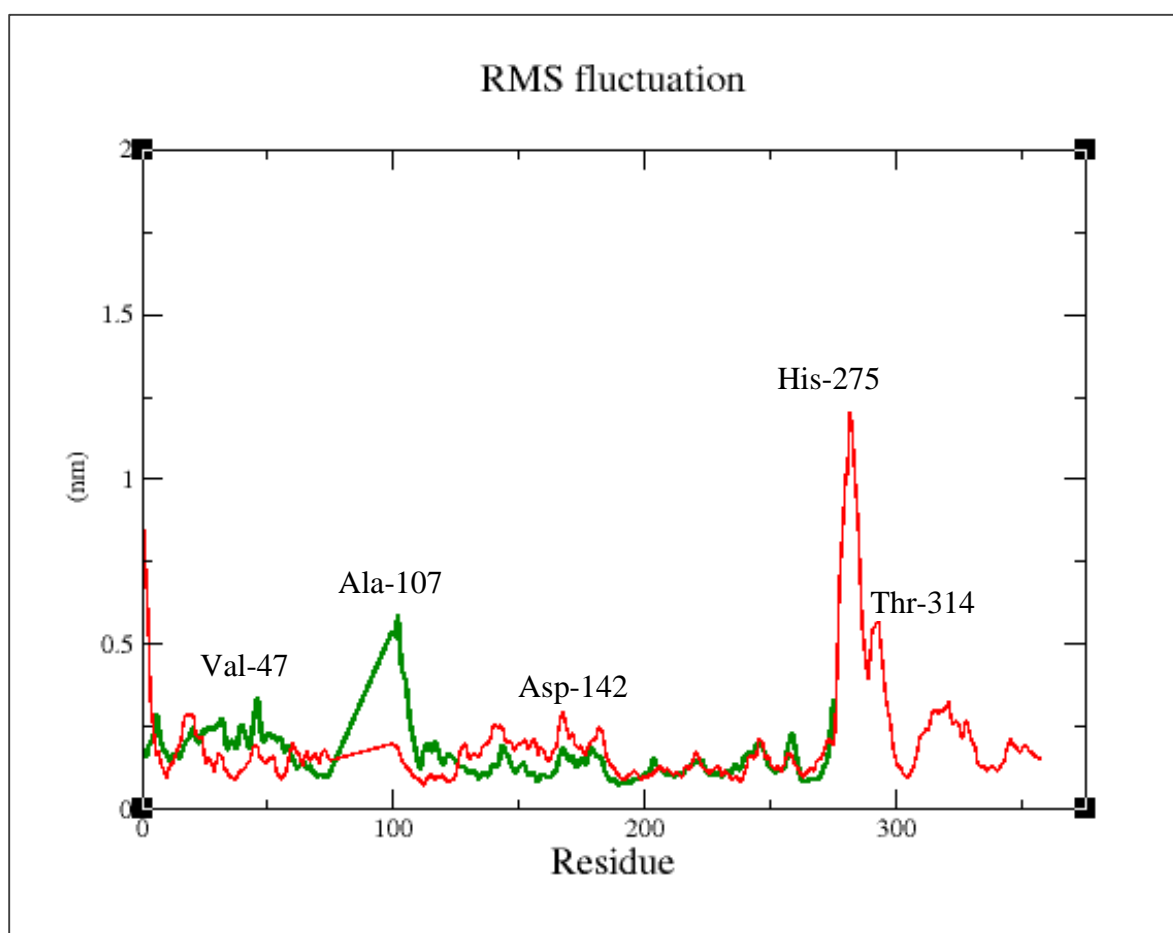


**Figure 26: RMSF observed within the Wild-type CABP4-IQ and Mutant CABP4-IQ docked complexes, including the identification of residues showing notable fluctuations. The red color corresponds to the fluctuation of residues in the docked Mutant CABP4-IQ complex, while the green color corresponds to the residual fluctuation in the docked complexes of Mutant CABP4-IQ.**

To further examine the trajectory stability of the docked complex, we conducted a hydrogen bond analysis using VMD. This analysis aimed to determine the interactions within the docked complex and its stability, as visualized in Figure 24. Our focus was on identifying the specific residues involved in forming hydrogen bonds crucial for the stability of the Wild-type CABP4-IQ docked complex. For this purpose, we calculated the H-bond occupancies, representing the proportion of time during which CABP4 protein atoms are involved in H-bonds with interacting residues in the IQ-MOTIF. The analysis showed that within the docked complex, the residues GLY162, GLU267, GLU210, and SER273 of CABP4 played a central role in forming hydrogen bonds. Similarly, the residues ASN2, TYR62, ARG75, and LYS73 of the IQ motif were also prominently involved in H-bond formation within the docked complex, as shown in Figure 27(a). This comprehensive analysis of hydrogen bonds emphasized the significance of the fourth EF domain of CABP4 in facilitating interactions with the IQ motif.

While analyzing the H-bond occupancy of the Mutant CABP4-IQ complex, it became evident that certain interactions were established. Specifically, the residues GLU192, Glu169, Lys342, and ARG100 of CABP4 formed H-bonds, as shown in Figure 27(b). However, despite their formation, these H-bonds did not contribute significantly to maintaining protein stability throughout the simulation. Likewise, the residues Lys40, Lys37, and Glu55 within the IQ motif displayed interactions with the docked complex. However, these particular H-bonds did not play a supportive role in facilitating the interaction between the Mutant CABP4 and the IQ motif within the docked complex.

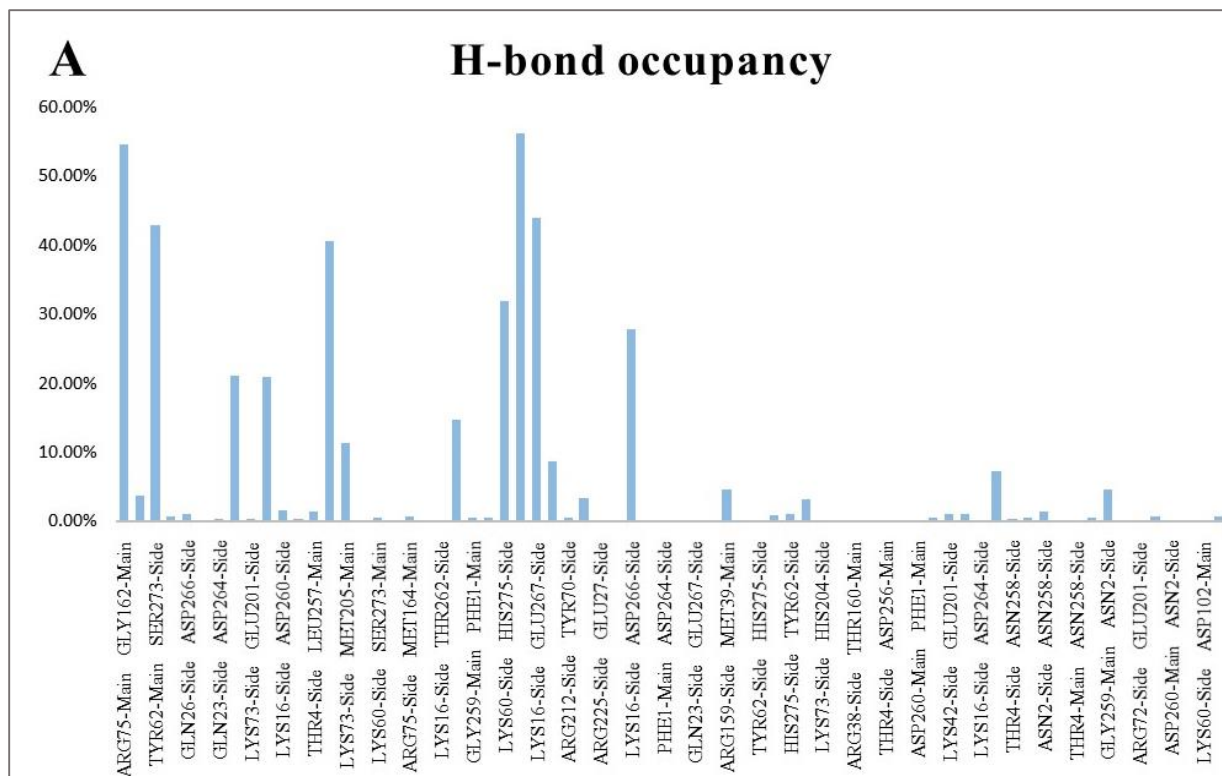


**Figure 27(a):** The assessment of H-bond occupancy for Wild-type CABP4-IQ docked complex for each interacting residue within their respective complexes throughout the simulation period.

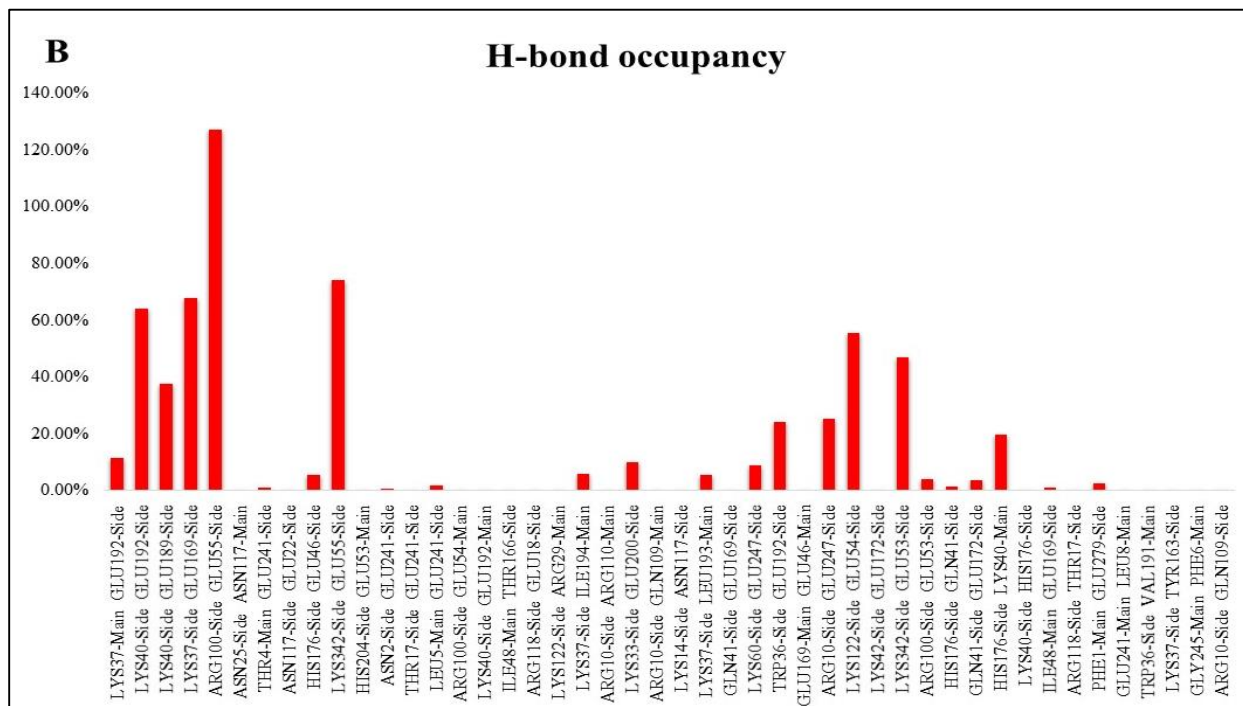


**Figure 27(b):** The assessment of H-bond occupancy for Mutant CABP4-IQ docked complex for each interacting residue within their respective complexes throughout the simulation period.

## Chapter 5

### 5 Discussion

The visual signaling mechanism in low-light conditions/dark relies on the activation of CABP4 by  $\text{Ca}^{2+}$ . CABP4 plays a crucial role in the regulation of the Cav1.4 channel, facilitating signal transmission from rod photoreceptors to the brain for visual processing. Changes in  $\text{Ca}^{2+}$  concentration can impact CABP4 behavior, resulting in delayed signal responses and potentially leading to night blindness. In this research work, the focus was on constructing the BRN ( $\text{Ca}^{2+}$  as the activator of CABP4), highlighting their combined importance in ensuring proper signal transmission within the visual system.

Three Biological Regulatory Networks (BRNs) were designed to investigate the role of  $\text{Ca}^{2+}$  and CABP4 in various visual signaling pathways. In the first BRN, which represents visual signaling in light conditions,  $\text{Ca}^{2+}$  and CABP4 were maintained in a low activation state, acting as positive signal regulators of visual signals. The first BRN was tested across varying light conditions, uncovering their specific effects on visual signaling responses. Under no light (0.0), the visual response was observed to decrease, while moderate light variation (0.5) caused a delay in signaling due to the GPCR activator's activation occurring subsequent to light stimulation. In contrast, heightened light intensity (1.0) resulted in an accelerated visual response by speeding up GPCR activation. These BRN results explain the complex relationship between light conditions and the dynamics of visual signaling.

Simulations of BRN for visual signaling in low light conditions/dark supported the hypothesis that  $\text{Ca}^{2+}$  plays a crucial role in the model's sensitivity. When GCAP (Guanylate Cyclase Activating Protein) was inhibited during low light conditions, positive signals were generated, leading to an increase in  $\text{Ca}^{2+}$  concentration, further activating CABP4. As a result,  $\text{Ca}^{2+}$  and CABP4 were in a hyperactive state, acting as activators of the visual signaling pathway. The third BRN was specifically designed to model night blindness. The simulations revealed that any alterations in  $\text{Ca}^{2+}$  and CABP4 levels resulted in the absence of visual signaling under low light conditions. Perturbing this BRN with changes in  $\text{Ca}^{2+}$  and CABP4 showed disrupted peaks in the network, leading to a low activation state of visual signaling.

To validate the target for night blindness, a comprehensive literature review was conducted, revealing CABP4 as the focus. The study explored the interaction of CABP4 with IQ-

motif through docking and simulations for both normal and disease states, aiming to confirm the accuracy of the docking results.

Due to the unavailability of the 3D structure of CABP4 and IQ motif that is the region of Cav1.4, we used the alpha-fold structure of Human-CABP4 *and* performed simulations to ensure stable conformation for the CABP4 protein. Additionally, the IQ-motif and Mutant-CABP4 were built using homology models and further simulated for stable conformation. After analyzing the structural stability of CABP4 proteins and their interaction with the IQ motif, both the wild-type CABP4 and Mutant-CABP4 were subjected to docking analysis using the HADDOCK software. Hydrogen bond interactions between specific residues were identified using the pdbsum online server. The results showed that the wild-type CABP4 formed favorable interactions with the IQ motif. Specifically, the fourth EF domain of CABP4 interacted with the IQ motif, and this interaction was found to be essential for keeping the channel open in dark or low light conditions for visual signaling.

However, in the case of the Mutant-CABP4, the docked complex revealed the absence of crucial interactions between the four EF domains of Mutant-CABP4 and the IQ-motif. As a consequence, Mutant-CABP4 failed to form a strong binding with the IQ motif, which might lead to improper regulation of channel activity. This improper regulation could ultimately result in night blindness, as the visual signaling pathway may not function appropriately under low light conditions. The validation process was extended through Molecular Dynamics (MD) simulations of the docked complexes. In the case of the Wild-type CABP4-IQ complex, the RMSD value remained within a stable range of 0.4 to 0.5 Å throughout the simulation period. In contrast, the Mutant CABP4-IQ complex displayed fluctuating RMSD values ranging between 0.2 to 0.8 Å. The subsequent analysis focused on understanding residual fluctuations during the simulation, accomplished through the calculation of RMSF. Notably fluctuating residues in the Wild-type CABP4-IQ complex included ALA3, VAL47, ARG100, ALA107, and HIS275. On the other hand, within the Mutant CABP4-IQ complex, residues like LYS60, ILE281, SER282, and THR314 exhibited high levels of fluctuation.

The investigation into hydrogen bond occupancy further elucidated the significance of the interaction between the IQ domain and the fourth EF domain of CABP4. This interaction emerged as a crucial factor for the proper functionality of rod photoreceptors.

## Chapter 6

### 6 Conclusions

The primary aim of this research was to validate CABP4 as a potential therapeutic target for addressing night blindness. To achieve this objective, a comprehensive biological regulatory network was designed and studied under varying light conditions. The outcomes of this investigation revealed a significant correlation between the concentrations of  $\text{Ca}^{2+}$  and CABP4, proving their influence on visual signaling. This observation was further validated by the sensitivity of BRN model, providing substantial support to our initial hypothesis. In situations of low light where there's an increase in  $\text{Ca}^{2+}$  levels, CABP4 becomes more active, resulting in prolonged heightened activity. This, in turn, magnifies the hyperactivity of visual signals, leading to increased responsiveness in low light conditions.

Conversely, when the concentration of CABP4 is disrupted due to mutations, its activity decreases, causing visual signals to stay inactive. This interruption in sending signals to the brain ultimately leads to the development of night blindness. Another important finding in this study was the understanding of how CABP4 regulates Cav1.4 by interacting with the IQ motif. Specifically, the presence of mutant CABP4 was seen to hinder the correct regulation of Cav1.4. This emphasizes once more the crucial role played by CABP4 in ensuring the proper functioning of the visual signaling pathway. The thorough investigation of how CABP4 and  $\text{Ca}^{2+}$  interact and affect visual signaling highlights a promising route for addressing night blindness. These discoveries don't just enhance our knowledge of eye health but also offer potential for developing new treatments to improve visual issues caused by CABP4-related problems. In wrapping up this study, it's important to target the CABP4 as a key role in preserving visual function and the need for more research to tap into its potential for clinical use in restoring clear vision.

## 7 References

1. Bootman MD, Collins TJ, Peppiatt CM, Prothero LS, MacKenzie L, De Smet P, et al. Calcium signalling--an overview. *Semin Cell Dev Biol.* 2001;12(1):3-10.
2. Song Z, Wang Y, Zhang F, Yao F, Sun C. Calcium Signaling Pathways: Key Pathways in the Regulation of Obesity. *Int J Mol Sci.* 2019;20(11).
3. Berridge MJ. The Inositol Trisphosphate/Calcium Signaling Pathway in Health and Disease. *Physiol Rev.* 2016;96(4):1261-96.
4. Wu HH, Brennan C, Ashworth R. Ryanodine receptors, a family of intracellular calcium ion channels, are expressed throughout early vertebrate development. *BMC Res Notes.* 2011;4:541.
5. Brini M, Cali T, Ottolini D, Carafoli E. Neuronal calcium signaling: function and dysfunction. *Cell Mol Life Sci.* 2014;71(15):2787-814.
6. Catterall WA. Voltage-gated calcium channels. *Cold Spring Harb Perspect Biol.* 2011;3(8):a003947.
7. Felix R, Calderón-Rivera A, Andrade A. Regulation of high-voltage-activated Ca(2+) channel function, trafficking, and membrane stability by auxiliary subunits. *Wiley Interdiscip Rev Membr Transp Signal.* 2013;2(5):207-20.
8. Weiss N, Zamponi GW. Trafficking of neuronal calcium channels. *Neuronal Signal.* 2017;1(1):Ns20160003.
9. Campiglio M, Flucher BE. The role of auxiliary subunits for the functional diversity of voltage-gated calcium channels. *J Cell Physiol.* 2015;230(9):2019-31.
10. Dolphin AC. Voltage-gated calcium channels and their auxiliary subunits: physiology and pathophysiology and pharmacology. *J Physiol.* 2016;594(19):5369-90.
11. Zamponi GW, Striessnig J, Koschak A, Dolphin AC. The Physiology, Pathology, and Pharmacology of Voltage-Gated Calcium Channels and Their Future Therapeutic Potential. *Pharmacol Rev.* 2015;67(4):821-70.
12. Lolley RN, Lee RH. Cyclic GMP and photoreceptor function. *Faseb j.* 1990;4(12):3001-8.
13. Kawai F, Horiguchi M, Suzuki H, Miyachi E. Na(+) action potentials in human photoreceptors. *Neuron.* 2001;30(2):451-8.
14. Waldner DM, Bech-Hansen NT, Stell WK. Channeling Vision: Ca(V)1.4-A Critical Link in Retinal Signal Transmission. *Biomed Res Int.* 2018;2018:7272630.
15. Varela C, Blanco R, De la Villa P. Depolarizing effect of GABA in rod bipolar cells of the mouse retina. *Vision Res.* 2005;45(20):2659-67.
16. Martemyanov KA, Sampath AP. The Transduction Cascade in Retinal ON-Bipolar Cells: Signal Processing and Disease. *Annu Rev Vis Sci.* 2017;3:25-51.
17. Rashwan R, Hunt DM, Carvalho LS. The role of voltage-gated ion channels in visual function and disease in mammalian photoreceptors. *Pflugers Arch.* 2021;473(9):1455-68.
18. Snellman J, Kaur T, Shen Y, Nawy S. Regulation of ON bipolar cell activity. *Prog Retin Eye Res.* 2008;27(4):450-63.
19. Chan CS, Guzman JN, Ilijic E, Mercer JN, Rick C, Tkatch T, et al. 'Rejuvenation' protects neurons in mouse models of Parkinson's disease. *Nature.* 2007;447(7148):1081-6.
20. Shin J, Kovacheva L, Thomas D, Stojanovic S, Knowlton CJ, Mankel J, et al. Ca(v)1.3 calcium channels are full-range linear amplifiers of firing frequencies in lateral DA SN neurons. *Sci Adv.* 2022;8(23):eabm4560.
21. Xu X, Marx SO, Colecraft HM. Molecular mechanisms, and selective pharmacological rescue, of Rem-inhibited CaV1.2 channels in heart. *Circ Res.* 2010;107(5):620-30.



22. Murphy CE, Wechsler AS. Calcium channel blockers and cardiac surgery. *J Card Surg.* 1987;2(2):299-325.
23. Flucher BE. Skeletal muscle Ca(V)1.1 channelopathies. *Pflugers Arch.* 2020;472(7):739-54.
24. Shaltiel L, Pappas C, Fenske S, Hassan S, Gruner C, Rötzer K, et al. Complex regulation of voltage-dependent activation and inactivation properties of retinal voltage-gated Cav1.4 L-type Ca<sup>2+</sup> channels by Ca<sup>2+</sup>-binding protein 4 (CaBP4). *J Biol Chem.* 2012;287(43):36312-21.
25. Lee A, Wang S, Williams B, Hagen J, Scheetz TE, Haeseleer F. Characterization of Cav1.4 complexes ( $\alpha$ 1.4,  $\beta$ 2, and  $\alpha$ 2 $\delta$ 4) in HEK293T cells and in the retina. *J Biol Chem.* 2015;290(3):1505-21.
26. Berger A, Lorain S, Joséphine C, Desrosiers M, Peccate C, Voit T, et al. Repair of rhodopsin mRNA by spliceosome-mediated RNA trans-splicing: a new approach for autosomal dominant retinitis pigmentosa. *Mol Ther.* 2015;23(5):918-30.
27. Moraru AD, Costin D, Iorga RE, Munteanu M, Moraru RL, Branisteanu DC. Current trends in gene therapy for retinal diseases (Review). *Exp Ther Med.* 2022;23(1):26.
28. Zeitz C, Kloeckener-Gruissem B, Forster U, Kohl S, Magyar I, Wissinger B, et al. Mutations in CABP4, the gene encoding the Ca<sup>2+</sup>-binding protein 4, cause autosomal recessive night blindness. *Am J Hum Genet.* 2006;79(4):657-67.
29. Park S, Li C, Haeseleer F, Palczewski K, Ames JB. Structural insights into activation of the retinal L-type Ca<sup>2+</sup> channel (Cav1.4) by Ca<sup>2+</sup>-binding protein 4 (CaBP4). *J Biol Chem.* 2014;289(45):31262-73.
30. Haeseleer F, Williams B, Lee A. Characterization of C-terminal Splice Variants of Cav1.4 Ca<sup>2+</sup> Channels in Human Retina. *J Biol Chem.* 2016;291(30):15663-73.
31. Wert KJ, Lin JH, Tsang SH. General pathophysiology in retinal degeneration. *Dev Ophthalmol.* 2014;53:33-43.
32. Littink KW, van Genderen MM, Collin RW, Roosing S, de Brouwer AP, Riemsdag FC, et al. A novel homozygous nonsense mutation in CABP4 causes congenital cone-rod synaptic disorder. *Invest Ophthalmol Vis Sci.* 2009;50(5):2344-50.
33. Jaffal L, Mrad Z, Ibrahim M, Salami A, Audo I, Zeitz C, et al. The research output of rod-cone dystrophy genetics. *Orphanet J Rare Dis.* 2022;17(1):175.
34. Khan NW, Kondo M, Hirianna KT, Jamison JA, Bush RA, Sieving PA. Primate Retinal Signaling Pathways: Suppressing ON-Pathway Activity in Monkey With Glutamate Analogues Mimics Human CSNB1-NYX Genetic Night Blindness. *J Neurophysiol.* 2005;93(1):481-92.
35. Haeseleer F, Imanishi Y, Maeda T, Possin DE, Maeda A, Lee A, et al. Essential role of Ca<sup>2+</sup>-binding protein 4, a Cav1.4 channel regulator, in photoreceptor synaptic function. *Nat Neurosci.* 2004;7(10):1079-87.
36. Taylor WR, Morgans C. Localization and properties of voltage-gated calcium channels in cone photoreceptors of *Tupaia belangeri*. *Vis Neurosci.* 1998;15(3):541-52.
37. Striessnig J, Bolz HJ, Koschak A. Channelopathies in Cav1.1, Cav1.3, and Cav1.4 voltage-gated L-type Ca<sup>2+</sup> channels. *Pflugers Arch.* 2010;460(2):361-74.
38. Gurkoff G, Shahlaie K, Lyeth B, Berman R. Voltage-gated calcium channel antagonists and traumatic brain injury. *Pharmaceuticals (Basel).* 2013;6(7):788-812.
39. Waldner DM, Giraldo Sierra NC, Bonfield S, Nguyen L, Dimopoulos IS, Sauvé Y, et al. Cone dystrophy and ectopic synaptogenesis in a *Cacna1f* loss of function model of congenital stationary night blindness (CSNB2A). *Channels (Austin).* 2018;12(1):17-33.
40. Laskowski RA, Jabłońska J, Pravda L, Vařeková RS, Thornton JM. PDBsum: Structural summaries of PDB entries. *Protein Sci.* 2018;27(1):129-34.
41. Maddox JW, Randall KL, Yadav RP, Williams B, Hagen J, Derr PJ, et al. A dual role for Ca(v)1.4 Ca(2+) channels in the molecular and structural organization of the rod photoreceptor synapse. *Elife.* 2020;9.
42. Yang PS, Johnny MB, Yue DT. Allosteric modulation of Ca<sup>2+</sup> channel modulation by calcium-binding proteins. *Nat Chem Biol.* 2014;10(3):231-8.

43. Woodruff ML, Sampath AP, Matthews HR, Krasnoperova NV, Lem J, Fain GL. Measurement of cytoplasmic calcium concentration in the rods of wild-type and transducin knock-out mice. *J Physiol.* 2002;542(Pt 3):843-54.
44. Park S, Li C, Ames JB. <sup>1</sup>H, <sup>15</sup>N, and <sup>13</sup>C chemical shift assignments of murine calcium-binding protein 4. *Biomol NMR Assign.* 2014;8(2):361-4.
45. Fallon JL, Baker MR, Xiong L, Loy RE, Yang G, Dirksen RT, et al. Crystal structure of dimeric cardiac L-type calcium channel regulatory domains bridged by Ca<sup>2+</sup>-calmodulins. *Proc Natl Acad Sci U S A.* 2009;106(13):5135-40.
46. Van Petegem F, Chatelain FC, Minor DL, Jr. Insights into voltage-gated calcium channel regulation from the structure of the CaV1.2 IQ domain-Ca<sup>2+</sup>/calmodulin complex. *Nat Struct Mol Biol.* 2005;12(12):1108-15.
47. Tan TE, Fenner BJ, Barathi VA, Tun SBB, Wey YS, Tsai ASH, et al. Gene-Based Therapeutics for Acquired Retinal Disease: Opportunities and Progress. *Front Genet.* 2021;12:795010.
48. Moore NA, Bracha P, Hussain RM, Morral N, Ciulla TA. Gene therapy for age-related macular degeneration. *Expert Opin Biol Ther.* 2017;17(10):1235-44.
49. Weng Y, Xiao H, Zhang J, Liang XJ, Huang Y. RNAi therapeutic and its innovative biotechnological evolution. *Biotechnol Adv.* 2019;37(5):801-25.
50. Aoki-Kinoshita KF, Kanehisa M. Gene annotation and pathway mapping in KEGG. *Methods Mol Biol.* 2007;396:71-91.
51. Karl S, Dandekar T. Jimena: efficient computing and system state identification for genetic regulatory networks. *BMC Bioinformatics.* 2013;14:306.
52. Di Cara A, Garg A, De Micheli G, Xenarios I, Mendoza L. Dynamic simulation of regulatory networks using SQUAD. *BMC Bioinformatics.* 2007;8:462.
53. Jumper J, Evans R, Pritzel A, Green T, Figurnov M, Ronneberger O, et al. Highly accurate protein structure prediction with AlphaFold. *Nature.* 2021;596(7873):583-9.
54. Webb B, Sali A. Comparative Protein Structure Modeling Using MODELLER. *Curr Protoc Bioinformatics.* 2016;54:5.6.1-5.6.37.
55. de Vries SJ, van Dijk M, Bonvin AM. The HADDOCK web server for data-driven biomolecular docking. *Nat Protoc.* 2010;5(5):883-97.
56. van Zundert GCP, Rodrigues J, Trellet M, Schmitz C, Kastrius PL, Karaca E, et al. The HADDOCK2.2 Web Server: User-Friendly Integrative Modeling of Biomolecular Complexes. *J Mol Biol.* 2016;428(4):720-5.
57. Rigsby RE, Parker AB. Using the PyMOL application to reinforce visual understanding of protein structure. *Biochem Mol Biol Educ.* 2016;44(5):433-7.
58. Van Der Spoel D, Lindahl E, Hess B, Groenhof G, Mark AE, Berendsen HJ. GROMACS: fast, flexible, and free. *J Comput Chem.* 2005;26(16):1701-18.
59. Hofmann KP, Lamb TD. Rhodopsin, light-sensor of vision. *Prog Retin Eye Res.* 2023;93:101116.
60. Black JB, Premont RT, Daaka Y. Feedback regulation of G protein-coupled receptor signaling by GRKs and arrestins. *Semin Cell Dev Biol.* 2016;50:95-104.
61. Palczewski K. Chemistry and biology of the initial steps in vision: the Friedenwald lecture. *Invest Ophthalmol Vis Sci.* 2014;55(10):6651-72.
62. Rehkamp A, Tänzler D, Iacobucci C, Golbik RP, Ihling CH, Sinz A. Molecular Details of Retinal Guanylyl Cyclase 1/GCAP-2 Interaction. *Front Mol Neurosci.* 2018;11:330.
63. Morshedian A, Woodruff ML, Fain GL. Role of recoverin in rod photoreceptor light adaptation. *J Physiol.* 2018;596(8):1513-26.
64. Guo Y, Miao Q, Zhang Y, Wang C, Liang M, Li X, et al. A novel missense creatine mutant of CaBP4, c.464G>A (p.G155D), associated with autosomal dominant nocturnal frontal lobe epilepsy (ADNFLE), reduces the expression of CaBP4. *Transl Pediatr.* 2022;11(3):396-402.

